DOI: 10.1002/ejoc.200601045

Polythiacrown Macro- and Gigantocycles with Chiral Diacetal Cores

Sarah Abramson,[a] Dvora Berkovich-Berger,[b] Shai Dagan,[c] Israel Goldberg,[a] Lara Golender,[a] Mikhail Grabarnik,[a] N. Gabriel Lemcoff,*[a,b] Sarah Weinman,[a] and Benzion Fuchs*[a]

Keywords: Macrocycles / Crown compounds / S ligands / Chiral diacetals / Tetraoxadecalins

We present a unique class of polythiacrown macro- and gigantocyclic[9] systems, consisting of ethylene 1,2-dithioglycol (ETG) to poly(ethylene thioglycol) (ETG_n) bridges over one to six diacetal units of the *cis*-1,3,5,7-tetraoxadecalin (TOD) type. The latter is a dissymmetric, chiral moiety, incorporating a cavity with built-in high electron lone pair concentration, serving as the "core" of chiral macrocyclic host systems with good inclusion ability of ions and polar molecules. We describe two approaches: (i) the reactions of the 2,6-bis(bromomethyl)-*cis*-TOD podand (**6**) with ETG or higher ETG_ns (**12**$_n$), in Cs_2CO_3 promoted processes, leading to the innate but uncontrolled formation of polythiacrown-TOD macrocycles having ETG/TOD ratios of 1:1 (**7**), 2:2 (**8**) and further 3:3–6:6 (**11**$_{1/m}$)[10] macrocycles *via* open dithiol intermediates, and (ii) judicious preparation, using K_2CO_3, of oligomeric dibromide intermediates with ETG_n:TOD ratios 1:2, 2:3 or 3:4 (**14**$_{n/m}$), which led (with further ETG_n) in a controlled way to the 2:2 (**8**$_n$), or 3:3, 4:4 and 6:6 (**11**$_{n/m}$) macro- and gigantocyclic systems. Altogether, the outcome of these processes depends on the relative concentrations of the reactants. Synthesis was accompanied by detailed (NMR and MS) spectroscopy. X-ray crystallographic analysis of a number of macrocycles, complemented by (MM & MD) computation, made possible valuable structural, stereochemical and conformational analysis. While sophisticated in their stereochemical features, these systems are readily prepared in enantiopure form and hold great promise of chemical reactivity in metal ion inclusion and molecular and chiral recognition.

Introduction

In a series of recent papers,[1–3] we have put forward the 1,3,5,7-tetraheterodecalin (THD) system (Scheme 1, top), as a paradigm of diacetal type polyheterobicyclic systems, holding promise for self assembly and complex formation, due to its lone pair electron carrying heteroatoms and their emplacement. These *trans*- or *cis*-THD molecules incorporate either the diacetal (X, X′ = O),[1] diaminal (X, X′ = NH)[2] or bis(oxaminal) (X = O, X′ = NH or vice versa)[3] groups and are offsprings of the respective tetrafunctionalized butanes with aldehydes (see Scheme 2 X, X′ = O).[1–3]

Of special interest is the dissymmetric *cis*-1,3,5,7-tetraheterodecalin stereoisomer, with the high lone-pair concentration in its cavity, as a building block for new chiral macromolecular host systems. A variety of such systems have thus been made available for exploration,[1–3] both experimentally and computationally, concerning structure, conformation, chirality, stereoelectronics and inclusion behavior. Thus, *cis*-tetraheterodecalin (THD) podands (type **1**) with functionalized 2,6-diaryl or -alkyl substituents have been prepared and these led to corresponding cyclophane, coronand and cryptand macrocycles. Indeed (Scheme 1, bottom), mounting, for example, aminomethylene units (Y = NH) on the oxygenated version of **1** (X = X′ = O) and using ethylene glycol bridges, gave rise to diazacrown-*cis*-tetraoxadecalin (TOD) macrocycles of type **2**, with very good and selective alkali and earth alkaline ion inclusion ability,[1e] whereas in the nitrogen series, a podand type derivative (**1**, X = X′ = NH, R = CH_2OH) was already able to bind Pb^{+2} with unprecedented strength.[2a] The mixed system (X = O, X′ = NH and vice versa),[3] was especially rich and interesting because of its diversification and ion template guided Dynamic Combinatorial Virtual Libraries.[3d,3e] Moreover, the combination of two to multiple *cis*-THD units with suitable spacers in type **3** macrocycles gave rise to interesting variegation, including stereoisomerism and chirality.[1g,3d–3e]

Nomenclature, Stereochemistry and Conformational Analysis

For clearness and to relate this with previous papers in the series[1f,j,k] as well as with early, mainly carbohydrate

[a] School of Chemistry, Tel-Aviv University, Ramat-Aviv, Tel-Aviv, 69978 Israel
Fax: +972-3-6409293
E-mail: bfuchs@post.tau.ac.il
[b] Department of Chemistry, Ben-Gurion University, P.O.Box 653, Beer-Sheva, 84105 Israel
Fax: +972-8-6461740
E-mail: lemcoff@bgu.ac.il
[c] Institute for Biological Research, P. O. Box 19, Ness-Ziona, 74100 Israel

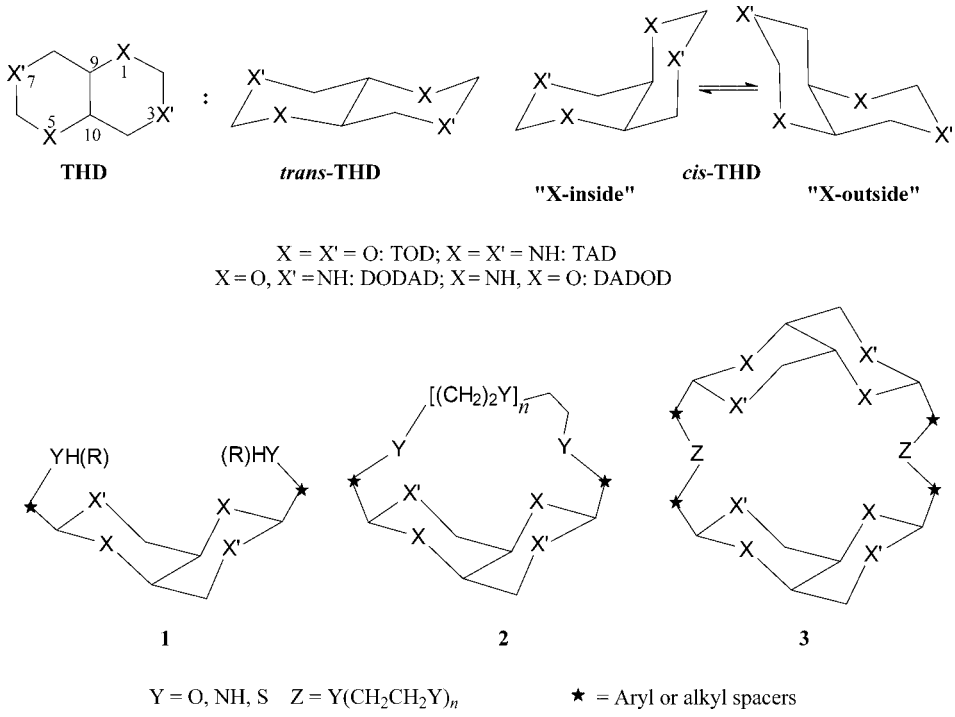

Scheme 1.

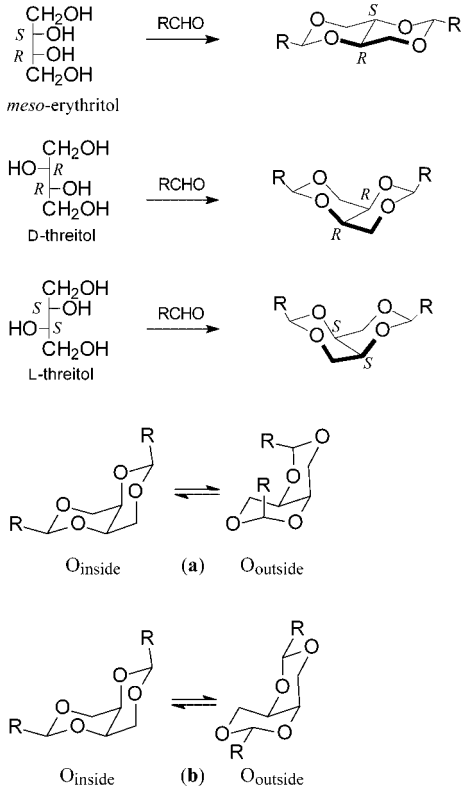

Scheme 2.

connected papers,[4] here is an outline of the principles by which these 1,3,5,7-tetraoxadecalin (TOD) systems are governed.

We use the 1,3,5,7-tetraoxadecalin (TOD) nomenclature and not the cumbersome CAS or carbohydrates namings and, when attaching the (poly)-ethylene thioglycol (ETG_n) spacers, we shall use, e.g., for the macrocyclic crowns **7** and **8** (cf. Scheme 4) the abbreviated terminology (1:1) ETG/TOD and (2:2) ETG/TOD, respectively.

As shown (Scheme 2), *trans*-TOD is formed from erythritol (preserving the *meso* character, *i* symmetry) and *cis*-TOD from *D*- or *L*-threitol (with preservation of chirality, C_2 symmetry). Also, due to a peculiar omission of the CIP rules, one can unequivocally assign configuration to any dissymmetric (C_2) *cis*-decalin (and similar) systems, *only* by 9,10-helicity specification. Thus, the (9*R*,10*R*)-*cis*-1,3,5,7-TOD O_{inside} and $O_{outside}$ stereoisomers (cf. Scheme 2, bottom, **a**) are (9,10-*M*)- and (9,10-*P*), respectively.

All TOD diastereomers occur in double chair conformations (the twist-boat and half-chair forms being way up in energy) and the two *cis*-TOD diastereomers are interconvertible as called for (Scheme 2, bottom), either (**a**) by conformational ring inversion or (**b**) by chemical isomerization (involving acetal opening and reclosure). The O_{inside} isomers are generally thermodynamically favored, with the understanding that an $O_{outside}$ isomer could be formed only if rendered thermodynamically more stable by judiciously effected substitution. In any case, if the condensing aldehyde introduces a relatively bulky R substituent (ethyl and up) on the 2,6-termini of the *cis*-TOD, it will necessarily wind up equatorially.

Thioethers and their role as ligands for the transition metals, are by now well-known and, especially crown polythioethers, are documented in numerous papers starting in the early 70's to recent years.[5–8,11,13,14] Recent extensive development of crown polythioether chemistry includes many potential uses, from ion selection, liquid crystals, to medical

purposes, etc.[6,8a] Newer and more efficient synthetic methods (put forward mainly by Kellogg et al.[7]) were based on the reactions of terminal dihalides with dithiols, sometimes by chain flanking procedures, using bases (mostly Cs_2CO_3) with DMF or THF as solvents. Catalytic, template ion techniques have also been reported for polythioethers,[8b] as were attempts to incorporate chiral core units.[7b,8b]

We aimed at the synthesis and study of oligo- and polymeric, along with macrocyclic systems based on diacetal (TOD) cores, separated by thioethylene spacers which have relatively tougher topological restraints.

There is bound to be much interest in how these thiacrown molecules will complex metal ions, polythioethers being known to have a great affinity for (late) transition metal cations.[11] In most complexes the metal ions are inside the polythiacrown ether, but in some they were found outside the ring. The strongly complexed Hg^{+2}, Pd^{+2}, and Pt^{+2} ions reached log *K* values of 20 or greater, since their interactions with the ligand may involve a certain degree of covalent bonding, while mixed oxygen-sulfur crown ethers, e.g., 1,10-dithio-18C6-complexed Ag^+ ion around log *K* = 4.

With all this in mind, we set out to make new chiral macrocycles consisting of poly(thiaethylene)-bridged *cis*-1,3,5,7-tetraoxadecalin (TOD) chiral core molecules, to probe how far one can go concerning ring size and to study the properties and behavior of such macrocycles. Results of earlier exploratory studies have been published in a Short Communication.[1g]

Results and Discussion

Synthetic Approaches

A number of approaches were considered for the synthesis of such macrocyclic *cis*-(TOD) systems, all naturally starting with threitol and various aldehydes[1j,1k] or dialdehydes.[11] We chose the former, from the recently described[1k] reaction (Scheme 3) of L-threitol (**4**) with judiciously substituted aldehydes to give (9*S*,10*S*)-*cis*-TOD podands bearing reactive centers in the 2 and 6 positions (**5**). The precursor of choice in the synthesis of our macrocycles was 2,6-bis(bromomethyl)-*cis*-1,3,5,7-tetraoxadecalin (**6**), which we had prepared and used before for the synthesis of other interesting crown compounds.[1k]

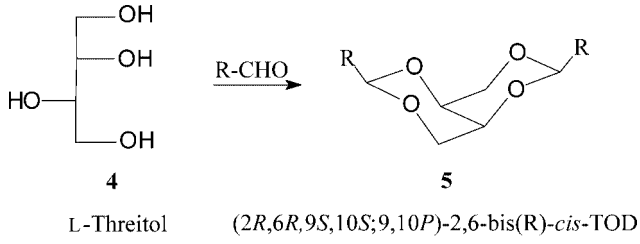

4 L-Threitol **5** (2*R*,6*R*,9*S*,10*S*;9,10*P*)-2,6-bis(R)-*cis*-TOD

Scheme 3.

The reaction of **6** with ethylene dithioglycol (ETG) (cf. Scheme 4) in Kellogg's reaction conditions,[7] i.e. Cs_2CO_3/DMF, to obtain the anticipated macrocycle (**7**), gave poor results and a spurious, even if interesting byproduct, to which the low yields were imputed, namely, the bis(oximinium) salt **X**, formed by interference of the solvent (DMF[12]).

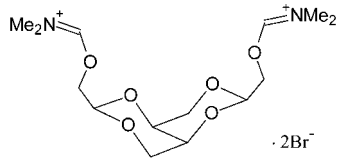

X

Salt X

Furthermore, while ordinary thiols reacted with **6** in ethanol/sodium ethoxide to give various **5** (e.g., R = CH_2SPh)

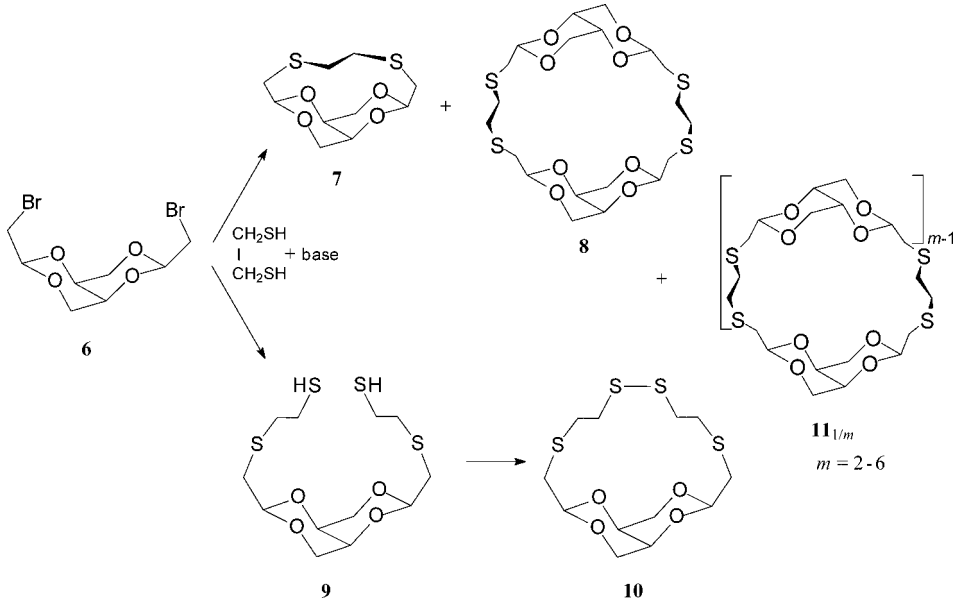

Scheme 4.[10]

in nearly quantitative yields, the reaction with ethylene dithioglycol (ETG) in similar conditions or in DMF with other bases provided no expected 2,6-bridged TOD (**7**).

Eventually, largely to prevent the formation of **X**, we ran the reactions in acetonitrile, which solved the problem and was then used routinely. Thus (Scheme 4), the reaction of the dibromide (**6**) with ETG in these conditions, viz., Cs_2CO_3/CH_3CN provided, mainly at room temperature, the basic crown dithioether (**7**) along with the 2:2 product (**8**) and accompanied by the higher (3:3, 4:4) ($\mathbf{11}_{1/3}$, $\mathbf{11}_{1/4}$)[10] analogues; higher molecular weight products were also observed, attesting to the formation of higher order (5:5 and 6:6) macrocycles in minute amounts. The (relative) yields were very much temperature dependent: at 20 °C the yields of **7** and **8** were 3 and 9%, respectively, while at 80° these changed to 20 and 4%, respectively, probably due to an entropic effect. Another expected dithiol intermediate (**9**) was also obtained but oxidized very rapidly in the presence of air to the corresponding disulfide (**10**). Following that and as anticipated, higher poly(ethylene thioglycols) (ETG_n) in MeCN and judiciously chosen conditions provided higher order homologous products, which made eventually possible assembly of entire libraries (Scheme 5).[10]

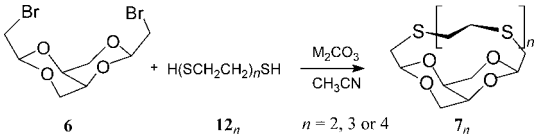

6 **12**$_n$ n = 2, 3 or 4 **7**$_n$

Scheme 5.[10]

Increasing the size of the dithiol, e.g. $\mathbf{12}_2$ and $\mathbf{12}_3$, provided in the chosen conditions better yields of the higher crown ($\mathbf{7}_2$ and $\mathbf{7}_3$) products, viz., 34 and 46% respectively. Interestingly, increase of concentrations of the reagents caused decrease in the yields (vide infra).

Attempts to improve the synthesis of the 1:1 macrocycles ETG_2:TOD ($\mathbf{7}_2$) and ETG_3:TOD ($\mathbf{7}_3$) by adding the dithiol in small portions (1/4 the total amount every 30 min) resulted only in minor improvements in yields. The ETG_3 and ETG_4 dithiols ($\mathbf{12}_3$ and $\mathbf{12}_4$, respectively) are not readily soluble in acetonitrile, so the reaction occurs with a low concentration of dithiol present in any case.

Furthermore (cf. Scheme 4), reaction of the dibromide (**6**) with a large excess of ETG under pure argon and careful workup, to avoid any oxidation, led safely to the 1:2 dithiol product **9**. The latter was the obvious precursor (in its reaction with **6**) of the [2:2] product **8**, which, in the new reaction conditions (Scheme 6), was isolated by chromatography in enantiopure (*S*,*S*;*S*,*S*)-form in ca. 20% yield followed by higher order [3:3 and 4:4] products $\mathbf{11}_{1/3}$ and $\mathbf{11}_{1/4}$.[10] The formation of those was rationalized as a stepwise macrocycle formation, involving intermediate oligomers $\mathbf{13}_{1/m}$, the occurrence of small amounts of which was established in the workup of the reaction mixture, based on NMR and mass spectrometry.

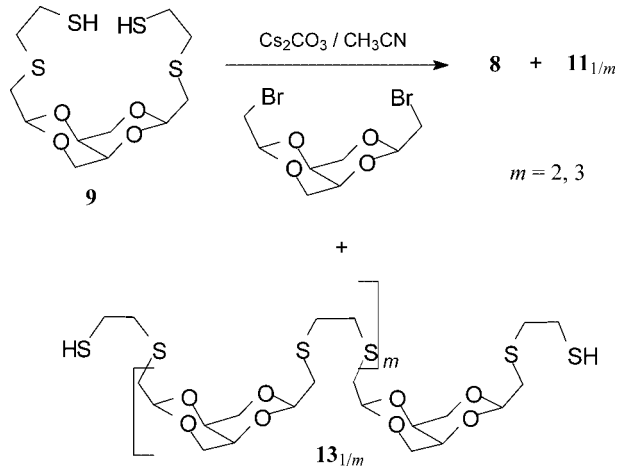

Scheme 6.[10]

The above described processes started with L-threitol to provide enantiopure (9*S*,10*S*)-*cis*-TOD products. Notably, when these reactions had been performed starting with the racemic (*S*,*S*)-**6**/(*R*,*R*)-**6** (originating in D,L-threitol), the reaction with ETG gave a racemic mixture of **7** accompanied by two diastereomers of **8**, namely *rac*-[(*R*,*R*;*R*,*R*-**8**) + (*S*,*S*;*S*,*S*)-**8**] with D_2 symmetry and *meso* (*S*,*S*;*R*,*R*-**8**) with C_{2h} symmetry (Scheme 7).

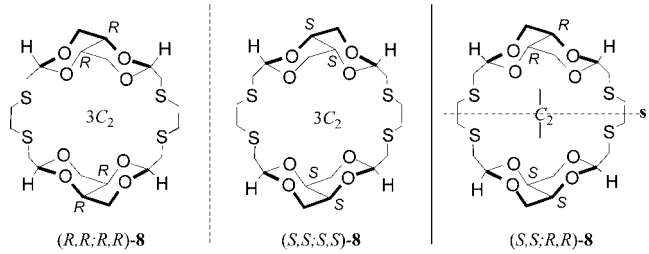

Scheme 7.

Evidently, for higher order oligomers and macrocyles, racemic TOD starting materials lead to difficultly resolvable mixtures of stereoisomeric products and therefore, only homochiral systems will be henceforth described, originating from either D- or, mostly L-threitol.

The bottom line of this first part of our paper is that taking a stochastic approach to the production of this type of systems conducts to mixtures of products which constitute, in fact, Combinatorial Libraries, as illustrated in Figure 1 for the basic process starting with D-threitol, and described in Scheme 4 and Scheme 6 for actual L-stemming cases. This is an exciting aspect we plan to pursue after having explored[11,3d,3e] it in related systems. Now, however, we are concerned with well elaborated, directed methods for achieving our macrocyclic diacetal-based systems, as described below.

Controlled Construction of Macro- and Gigantocycles[9]

A rational, controlled methodology for the construction of polythia macromolecules was worked out by proceeding

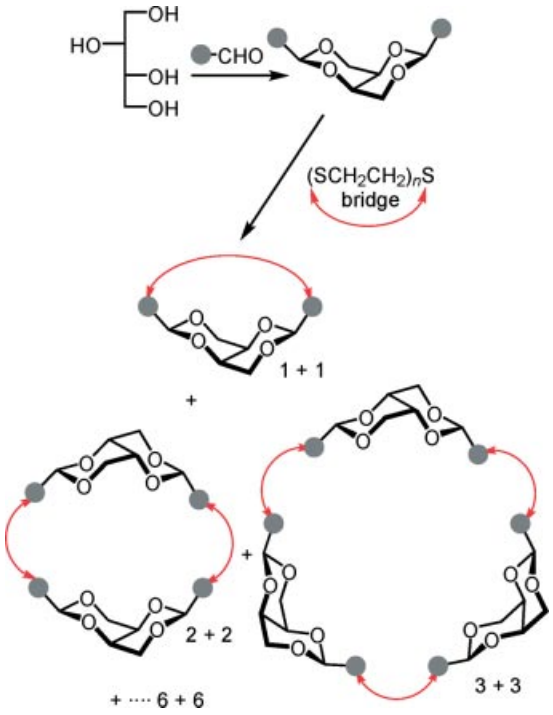

Figure 1. Schematic formation of libraries of homochiral macrocyclic polythiacrown-1,3,5,7-TODs starting from D-threitol, substituted aldehydes and polyetyhylene thioglycols.

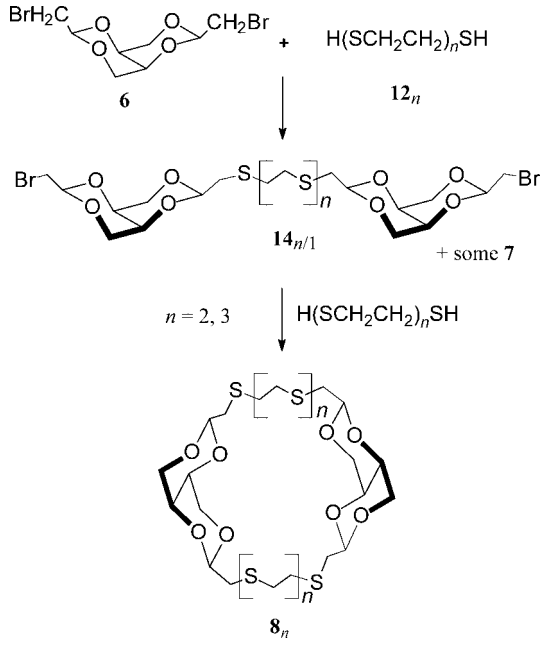

Scheme 8.[10]

via bis(bromomethyl)-terminated TOD oligomers and by using two consecutive procedures, which are controlled by modifying the relative amount of reactants. The initial process was the base catalysed reaction of 2,6-bis(bromomethyl)-*cis*-TOD (**6**) *in excess* with ethylene dithioglycol ($\mathbf{12}_1$) (Scheme 8), to afford, next to small amounts of the ETG macrocycles (**7**, **8**, $\mathbf{11}_{1/m}$) the oligomeric compound with bromomethyl termini ($\mathbf{14}_{n/1}$).[10]

Analogously, the ETG_n multiples ($\mathbf{12}_{2–3}$) provided the respective oligomers ($\mathbf{14}_n$), followed by their judicious ring closing condensation to the macrocyclic systems ($\mathbf{8}_n$) as well as higher macrocycles (see below).

In this approach, the main feature was the use of solid potassium carbonate as basic promoting agent. Depending on the reaction conditions, which were optimized in most cases, the desired oligomeric product was *preferentially* obtained and the eventual outcome was, in fact, more variegated and interesting.

This is exemplified in Scheme 9 for the reaction of a twofold excess of dibromomethyl-TOD (**6**) with triethylene thioglycol (ETG_3, $\mathbf{12}_3$), which provided in addition to the expected 1:2 ETG_3:TOD open chain compound ($\mathbf{14}_{3/1}$),[10] the higher 2:3 and 3:4 oligomers ($\mathbf{14}_{3/2}$ and $\mathbf{14}_{3/3}$, respectively), albeit in lower yields.

The triethylene thioglycol (ETG_3) starting material contained ca. 5% of tetraethylene thioglycol (ETG_4) and was difficult to purify (see also ref.[16]). This resulted in small amounts of ETG_4 products in the reactions with ETG_3. In the smaller macrocycles, byproducts of such origin could be easily separated out by chromatography.

The following, final and exciting step is a condensation/cyclization reaction of the dibromo-terminated oligomers with the respective ETG_n in a *one to one ratio* of reactants. Thus, as depicted in Scheme 10, the condensation of the 1:2 oligomer ($\mathbf{14}_{3/1}$) with the ETG_3 dithiol afforded the macrocyclic 2:2 ($\mathbf{8}_3$) and gigantocyclic 4:4 ($\mathbf{11}_{3/4}$) products.

In a similar way (Scheme 11), the 2:3 oligomer ($\mathbf{14}_{3/2}$) gave the 3:3 macrocycle ($\mathbf{11}_{3/3}$) and the respective ultracycle 6:6 ($\mathbf{11}_{3/6}$) (with more than 100 atoms in its perimeter – using Vögtle's terminology[9]). Altogether, the size of macrocycle formed was efficiently controlled by manipulating the initial concentrations of the reagents, namely, dilute reaction conditions provided higher yields of the smaller macrocycles and vice versa.

To assess the generality of the approach, we used a different dithiol spacer in the last cyclization steps and succeeded to prepare macrocycles with ETG_n bridges of mixed size, as demonstrated by the preparation of the $2_{2,3}$:2 macrocycle ($\mathbf{15}_{2,3/2}$) (Scheme 12) in the reaction of $\mathbf{14}_{3/1}$ with $\mathbf{12}_2$. To be sure, the same major product ($\mathbf{15}_{2,3/2}$) was obtained (Scheme 12, bottom)[10] when the starting materials were $\mathbf{14}_{2/1}$ and $\mathbf{12}_3$ instead of the ones at the top, demonstrating the permutability of the reaction (although the trace byproducts obtained were not the same, as expected).

Furthermore, in all above described processes, disulfide macrocycles were observed and in two cases (**10** – cf. Scheme 4 – and $\mathbf{10}_3$) they were isolated. These disulfide crowns, obtained first as spurious byproducts, are interesting,[11] readily accessible and potentially useful thiacrown macrocycles. In this context and as already discussed with regard to Schemes 3 and 5, the use of an oxygen free atmosphere is a critical factor for all the reactions. Even under rigorous conditions it is difficult to prevent completely the formation of the disulfides arising from the oxidation of the dithiols in the reaction mixture. Thus, even the basic and

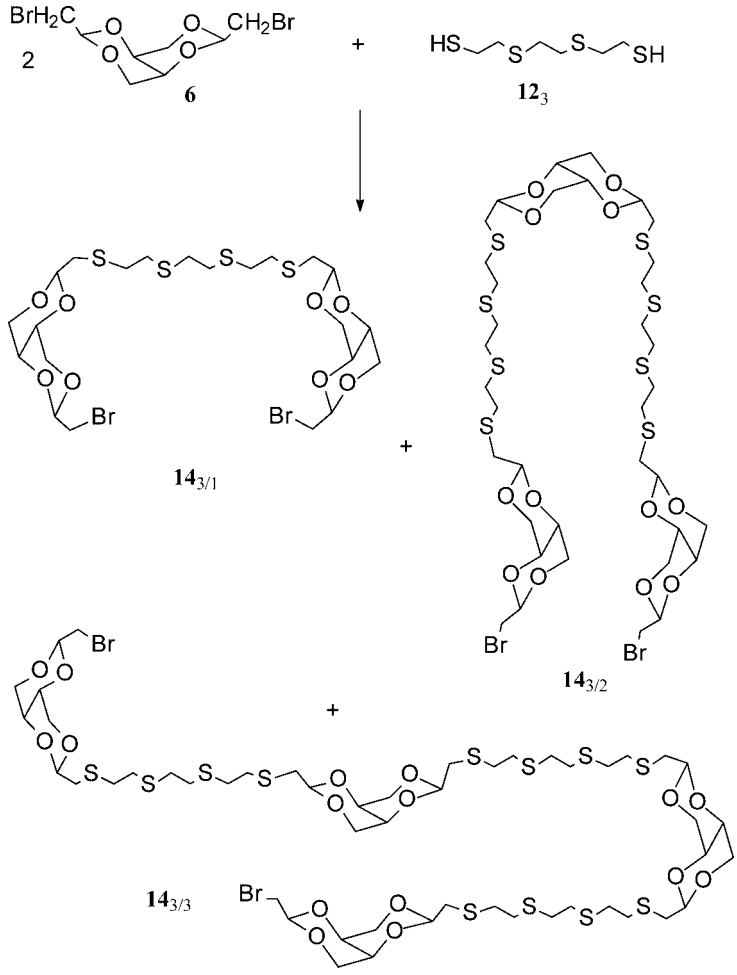

Scheme 9.[10]

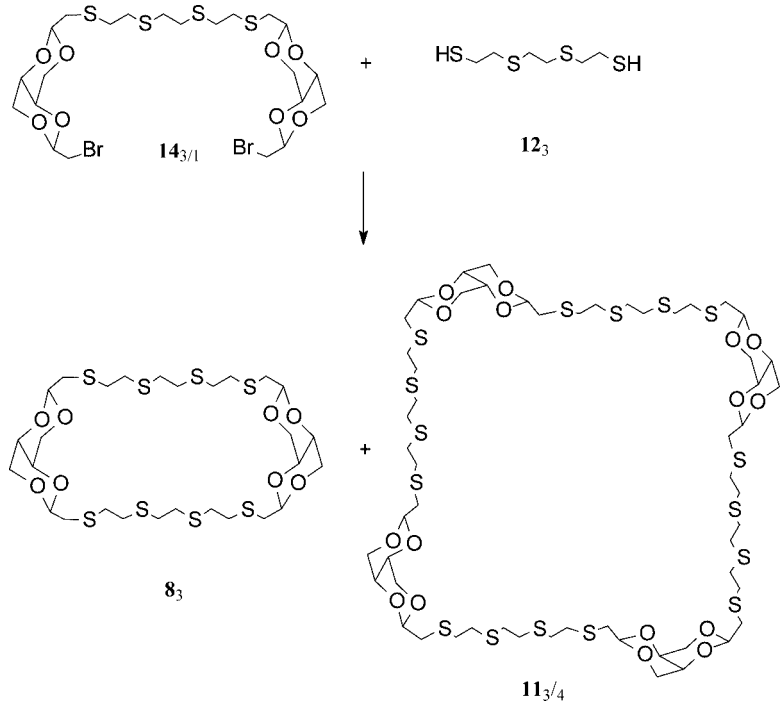

Scheme 10.[10]

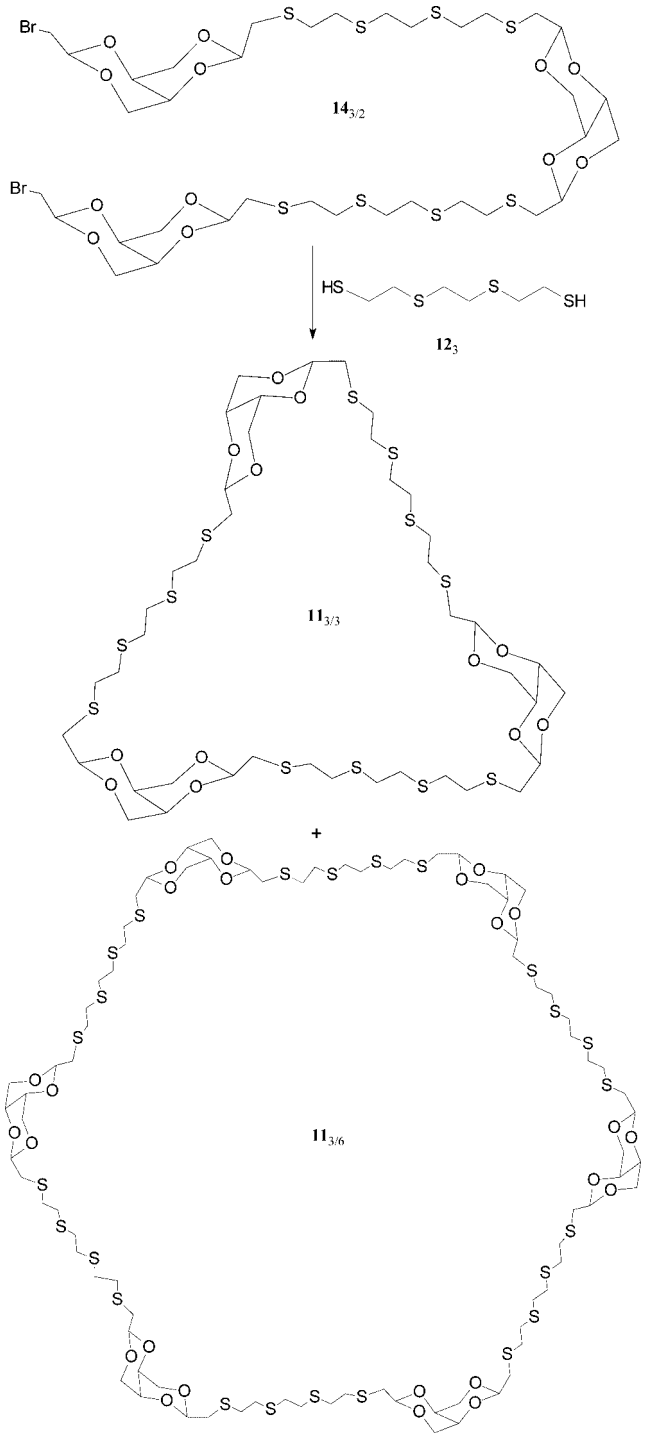

Scheme 11.[10]

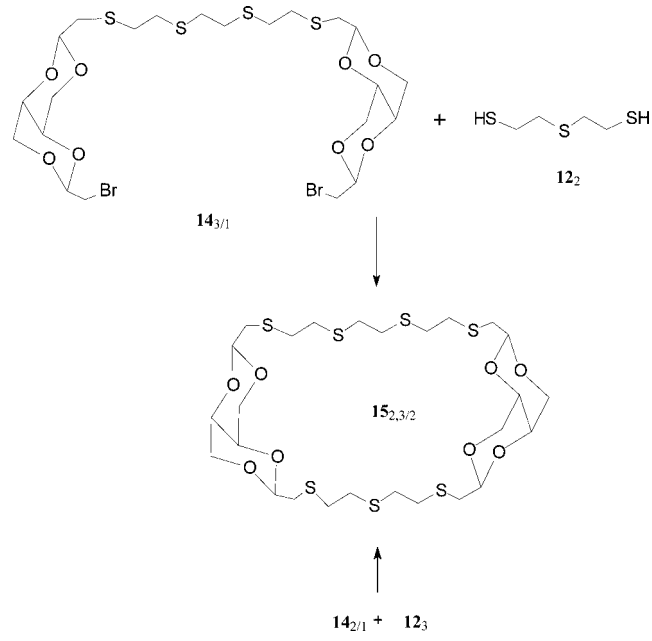

Scheme 12.[10]

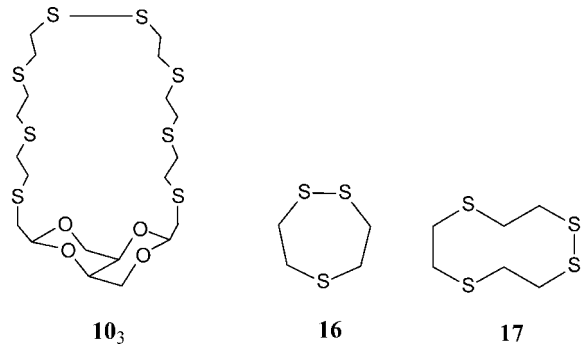

Table 1. ETG_n-bridged TOD* oligomers (O) and macrocycles (M).[10]

ETG_n:TOD	ETG	ETG_2	ETG_3	ETG_4
1:1M ($\mathbf{7}_n$)	$\mathbf{7}$✓	$\mathbf{7}_2$✓	$\mathbf{7}_3$✓	$\mathbf{7}_4$✓
2:2M ($\mathbf{8}_n$)	$\mathbf{8}$✓	$\mathbf{8}_2$✓	$\mathbf{8}_3$✓	
3:3M ($\mathbf{11}_{n/3}$)	$\mathbf{11}_{1/3}$✓	$\mathbf{11}_{2/3}$✓	$\mathbf{11}_{3/3}$✓	
4:4M ($\mathbf{11}_{n/4}$)	$\mathbf{11}_{1/4}$#	$\mathbf{11}_{2/4}$✓	$\mathbf{11}_{3/4}$✓	
6:6M ($\mathbf{11}_{n/6}$)	$\mathbf{11}_{1/6}$#	$\mathbf{11}_{2/6}$✓	$\mathbf{11}_{3/6}$✓	
1:2O ($\mathbf{14}_{n/1}$)		$\mathbf{14}_{2/1}$✓	$\mathbf{14}_{3/1}$✓	
2:3O ($\mathbf{14}_{n/2}$)	$\mathbf{14}_{1/2}$#	$\mathbf{14}_{2/2}$✓	$\mathbf{14}_{3/2}$✓	$\mathbf{14}_{3/3}$#
3:4O ($\mathbf{14}_{n/3}$)	($\mathbf{14}_{1/3}$)#	($\mathbf{14}_{2/3}$)✓	($\mathbf{14}_{3/3}$)✓	
$2_{2,3}$:2M		$\mathbf{15}_{2,3/2}$		
2:1M	$\mathbf{10}$✓		$\mathbf{10}_3$✓	

*ETG = ethylene dithioglycol (**12**) and its *n* multiples ($\mathbf{12}_n$); TOD = 2,6-dimethylene-*cis*-1,3,5,7-tetraoxadecalin; ✓ = isolated, # = observed.

very stable disulfides of ETG_2 (**16**) and of ETG_3 (**17**) were found in the respective reaction mixtures and could be readily purified and characterized.

Table 1 is a display and glossary of all the oligomeric and macrocyclic systems secured in this work, starting from bis(bromomethyl)-*cis*-TOD (**6**) and ETG_n ($\mathbf{12}_n$) bridges, as described above, in general form (Schemes 3, 4, 5, 6, and 7) and then (Schemes 8, 9, 10, and 11) specifically for the triethylene thioglycol case.

We turn now to a, first worrying but then, highly interesting feature in all the above described processes, viz., the dynamic behaviour of the ETG_n containing systems. Thus, for example, in the synthesis of the 2:2 ETG_2:TOD ($\mathbf{8}_2$) macrocycle from the 1:2 ETG_2:TOD oligomer ($\mathbf{14}_{2/1}$) with ETG_2 ($\mathbf{12}_2$), a small amount of 1:1 ETG_2:TOD ($\mathbf{7}_2$) was also formed. Or, when preparing the *mixed* 2:2 macrocycle

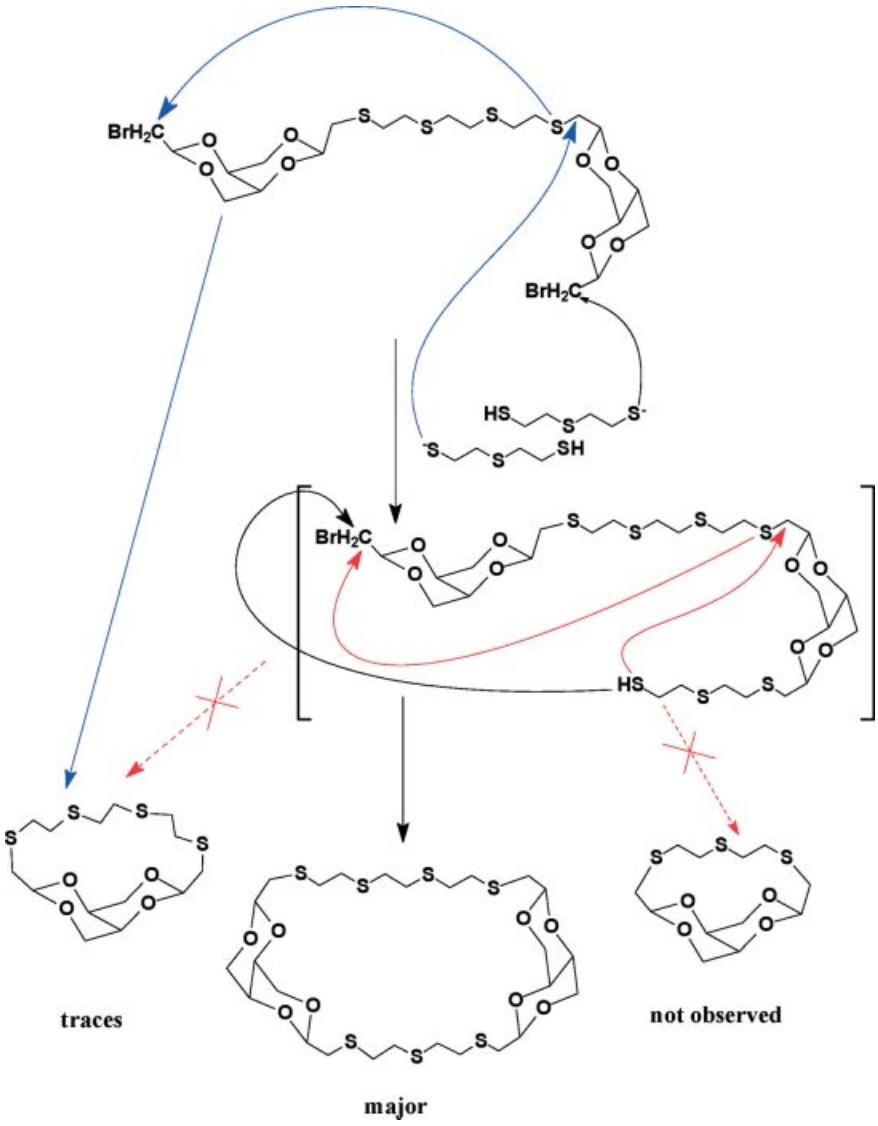

Scheme 13.

($\mathbf{15}_{2,3/2}$) by reacting 1:2 ETG_2:TOD ($\mathbf{14}_{2/1}$) with ETG_3 ($\mathbf{12}_3$), 1:1 ETG_2:TOD ($\mathbf{7}_2$) was again isolated, but no 1:1 ETG_3:TOD was observed.

Conversely, the transposed counterpart reaction of 1:2 ETG_3:TOD ($\mathbf{14}_{3/1}$) with ETG_2 ($\mathbf{12}_2$) gave ($\mathbf{15}_{2,3/2}$) accompanied only by 1:1 ETG_3:TOD and no 1:1 ETG_2:TOD was observed. A tentative reaction outline is presented in Scheme 13. This "internal metacyclization" occurred in all cases we examined also with larger, e.g., 3:2 oligomers from which 1:1 and 2:2 macrocycles were also obtained as minor byproducts.

This behavior is reminding of related exchange processes described a long time ago by Ochrymowycz et al.[13] and recently by the Sanders and Otto.[11] In Scheme 13 we offer a tentative mechanistic scheme for the 1:2-ETG_3:TOD + ETG_2 case, in which we propose that any side reaction occurs before the formation of the intermediate oligomer and not from it. In fact, this is yet another aspect of a general phenomenon of diversification in poly-ETG systems which will be dealt with in a forthcoming publication.[16]

Spectrometric (^{1}H- and ^{13}C-NMR and MS) Analysis

Our main tools in the structural determination of all above-mentioned products were ^{1}H- and ^{13}C-NMR spectroscopy, the assignments were made by 2D and NOE techniques. For a comparative survey of these results see in Tables 2 and 3.

The spectra are conspicuously similar, with small systematic differences, making NMR a valuable diagnostic tool for these systems. The different sizes of the macrocycles are well detectable by the chemical shift of the acetal (**2**, **6**) proton (cf. Table 3); thus, for e.g., the 1:1 macrocycles **7** and $\mathbf{7}_2$ (along with the $1{:}2_1$ ring, **10**) δ = 4.9–5.1 ppm is observed and ca. 4.75 ppm for the higher $\mathbf{7}_3$ and $\mathbf{7}_4$ homologues along

Table 2. ^{1}H- and ^{13}C-NMR spectroscopic data of TOD podands and ETG$_n$/TOD oligomers ($CDCl_3$)[a].[10]

Cpd.	Position Splitting	2,6 ($^3J_{2,11}$)	4,8 ($^2J_{4ax,4eq}$; $J_{4ax,10}$) [$^3J_{4eq,10}$]	9,10	11$_{term}$ ($^2J_{11A,11B}$)	11$_{int}$, 13, 13'	14, 14' 15, 15' 17, 17'
5 R = CH_2 SPh	^{1}H δ_{ppm}, J_{Hz}	4.74 (dd) (5.0)	**ax**: 3.87 (dd) (12.7; 1.3) **eq**: 4.20 (d)	3.60 (br. m)	3.24 (d)		7.3 (m) (arom.)
	^{13}C, δ	100.51	69.57	69.57	37.50	126.12; 128.97	
6	^{1}H δ_{ppm}, J_{Hz}	4.83 (dd) (5.0)	**ax**: 3.93 (dd) (12.7; 1.3) **eq**: 4.24 (d)	3.67 (br. m)	3.44 (d) (CH_2Br)		
	^{13}C, δ	100.11	69.50	69.50	30.95		
14$_{2/1}$	^{1}H δ_{ppm}, J_{Hz}	4.82 (t)$_{term}$ 4.75 (t)$_{int}$	**ax**: 3.92 (12.8, 1.6) **eq**: 4.21 [0.6]	3.66	3.44 (CH_2Br)	2.85 (m)	
14$_{3/1}$	^{1}H δ_{ppm}, J_{Hz}	4.82 (t)$_{term}$, 4.75 (t)$_{int}$	**ax**: 3.92 (12.8, 2.0) **eq**: 4.21 [1.0]	3.67, 3.65 (m)	3.45 (CH_2Br)		2.85 (m)
	^{13}C δ_{ppm}	102.2$_{term}$, 100.1$_{int}$	69.7, 69.6 69.4, 69.3		31.1 (CH_2Br)		35.4, 32.9, 32.14, 32.06
14$_{2/2}$	^{1}H δ_{ppm}, J_{Hz}	4.82 (t)$_{term}$, 4.75, 4.74 (t)$_{int}$	**ax**: 3.92 (b) (12.6) **eq**: 4.21, 4.18 [0.6]	3.65 (b)	3.45		2.85 (m)
14$_{3/2}$	^{1}H δ_{ppm}, J_{Hz}	4.82 (t)$_{term}$, 4.75, 4.74 (t)$_{int}$	**ax**: 3.92, 3.91 (12.8, 2) **eq**: 4.21, 4.18 3.90 [1]	3.65 (m)	3.45 (CH_2Br)		2.85 (m)
	^{13}C, δ	102.2$_{term}$, 100.1$_{int}$	69.7, 69.6 br., 69.5, 69.4, 69.3		31.1 (CH_2Br)		35.5, 35.4, 33.0 br., 32.2 br., 32.1 br.,
14$_{2/3}$	^{1}H δ_{ppm}, J_{Hz}	4.82 (t)$_{term}$, 4.75 (t)$_{int}$	**ax**: 3.91 (br.) (12.6) **eq**: 4.21, 4.18 [0.6]	3.65 (m)	3.45 (CH_2Br)		2.85 (m)
14$_{3/3}$	^{1}H δ_{ppm}, J_{Hz}	4.83 (t)$_{term}$, 4.76, 4.74 (t)$_{int}$	**ax**: 3.92, 3.91 (12.6, 2) **eq**: 4.21, 3.90 4.18 [1]	3.65 (m)	3.45 (CH_2Br)		2.85 (m)
	^{13}C δ_{ppm}	102.2$_{term}$, 100.1$_{int}$	69.7, 69.6 br., 69.5, 69.4, 69.3		31.1 (CH_2Br)		35.5, 35.4, 32.9 br., 32.2 br.

[a] The primed atoms are related by C_2 symmetry to the corresponding ones in the oligomer chain; d = doublet; b = broad; m = multiplet; term = terminal; int = internal; **eq** = equatorial, **ax** = axial protons.

with the larger (2:2–6:6) macrocycle, which are less strained; the $^1H_{2,6}$ atoms are normally shielded (comparable to the internal $^1H_{2,6}$ in the open podand series, cf. Table 2), the corresponding signal appears upfield-shifted. For carbon, i.e., $^{13}C_{2,6}$, the trend is just the other way round.

Mass Spectrometry

All new small molecules were analysed by regular HR-MS techniques, while the larger molecular systems (>1000 Daltons) were analyzed by MALDI-TOF (matrix-assisted laser desorption ionization – time of flight) mass spectrometry, which allows analysis of such high-molecular weight compounds with high sensitivity.

Two matrices (and sometimes none) were found useful for these systems: DHB (2,5-dihydroxybenzoic acid) and Dithranol (1,8,9-trihydroxyanthracene). Table 4 provides the most significant peaks obtained in the relevant spectra using DHB. In some cases silver ion was added in the form of silver triflate to improve the ionization process as frequently done with (particularly sulfur containing) polymers in MALDI analyses.

Table 3. ^{1}H- and ^{13}C-NMR spectroscopic data of ETG$_n$/TOD macrocycles, ($CDCl_3$, δ_{ppm}, J_{Hz}).[10]

Cpd. (ETG$_n$: TOD)	Position Splitting	2,6 δ (spl)[‡] ($^3J_{2,11}$)	4,8 δ ($^2J_4$;$^3J_{4ax,10}$) [$^3J_{4eq,10}$][‡]	9,10 δ (spl)[b]	11,11'[a] δ (spl)[b]	13, 13' – 17-17'[a] δ (spl)[b]
7 (1_1:1)	^{1}H	5.12 (d) (3.8)	**ax**: 3.87 (d) (12.3;) **eq**: 4.24 (dd) [1.5]	3.60 (br. m)	2.66 (dd) 3.19 (d) (14.6)	2.88 (m), 3.84 (m)
	^{13}C	98.30	69.18	68.54	32.74; 36.66	
7$_2$ (1_2:1)	^{1}H	4.91 (dd) (3.5; 4.2)	**ax**: 3.87 (dd) (12.7; 1.0) **eq**: 4.22 (dd) [0.7]	3.63 (br. m)	2.82 (dd) 2.92 (dd) (15.2)	2.9 (m), 3.2 (m)
	^{13}C	99.15	68.93	68.93	29.67; 32.64; 34.61; 35.69	
7$_3$ (1_3:1)	^{1}H	4.79 (t) (5.0)	**ax**: 3.90 (dd) (12.4; 1.0) **eq**: 4.16 (d)	3.66 (br. m)	2.75 (dd) 2.86 (dd) (15.2)	2.8 (m)
	^{13}C	102.32	69.34	68.91	31.56; 32.19; 33.55	
7$_4$ (1_4:1)	^{1}H	4.77 (t) (4.6)	**ax**: 3.92 (dd) (12.5; 1.3) **eq**: 4.18 (d)	3.66 (br. m)	2.8 (m)	
	^{13}C	103.80	69.65	69.48	31.78; 31.92; 32.52; 34.64	
S,S;S,S-**8** (2_1:2)	^{1}H	4.74 (dd) (3.7; 6.4)	**ax**: 3.86 (dd) (12.6; 0.9) **eq**: 4.24 (d)	3.63 (br. m)	2.69 (dd) 2.91 (dd) (14.8)	2.80 (m) 3.12 (m)
	^{13}C	103.21	69.46	69.18	32.05; 33.72	
meso S,S;R,R-**8** (2_1:2)	^{1}H	4.75 (t) (5.1)	**ax**: 3.88 (br. d) (12.7;) **eq**: 4.21 (d)	3.62 (br. m)	2.82 (d)	2.96 (m)
	^{13}C	103.18	69.66	69.44	32.53; 34.65	
S,S;S,S-**8**$_2$ (2_2:2)	^{1}H	4.76 (t) (4.9)	**ax**: 3.90 (dd) (12.5; 1) **eq**: 4.18 (d)	3.63	2.8 – 3.0 (br. m)	
	^{13}C	102.6	69.5	69.3	35.0, 32.7, 31.5	
S,S;S,S-**8**$_3$ (2_3:2)	^{1}H	4.76 (t) (4.8)	**ax**: 3.90 (dd) (12.5; 1) **eq**: 4.18 (d)	3.64	2.7 – 3.0 (br. m)	
	^{13}C	102.3	69.5	69.3	35.2, 32.8, 32.1, 32.0	
10 (2_1:1)	^{1}H	4.89 (t) (4.3)	**ax**: 3.86 (dd) (12.3; 1.0) **eq**: 4.21 (d)	3.64 (br. m)	2.83 (d)	3.1 (m)
	^{13}C	99.93	69.00	68.61	31.18; 33.37; 37.77	
10$_3$ (2_3:1)	^{1}H	4.77 (t) (4.8)	**ax**: 3.90 (dd) (12.5; 1.5) **eq**: 4.18 (d) (12.5)	3.64 (br. m)	2.83 – 3.1 (m)	
	^{13}C	102.3	69.5	69.3	38.9; 35.0; 32.8	
11$_{1/3}$ (3_1:3)	^{1}H	4.75 (t) (4.9)	**ax**: 3.90 (br. d) (12.6) **eq**: 4.18 (d)	3.66 (br. m)	2.82 (d)	2.88 (br. m)
	^{13}C	102.27	69.5 (b)	69.5 (b)	34.7, 32.5	
11$_{2/4}$ (4_2:4)	^{1}H	4.74 (t) (4.9)	**ax**: 3.91 (br. d) (12.5) **eq**: 4.17 (d)	3.65	2.7 – 2.9 (br. m)	
11$_{3/4}$ (4_3:4)	^{1}H	4.75 (t) (5.0)	**ax**: 3.91 (dd) (12.5; 1) **eq**: 4.18 (d)	3.65	2.7 – 2.9 (br. m)	
	^{13}C	102.4	69.6	69.4	35.5, 32.9, 32.3, 32.2	
11$_{2/3}$ (3_2:3)	^{1}H	4.75 (t) (5.0)	**ax**: 3.90 (br. d) (12) **eq**: 4.18 (d)	3.64 (m)	2.7 – 2.9 (br. m)	
	^{13}C	102.27	69.6	69.4	35.4, 32.9, 32.0, 29.7	

Table 3. *(continued)*

Cpd. (**ETG$_n$:TOD**)	Position Splitting	2,6 δ (spl)* ($^3J_{2,11}$)	4,8 δ ($^2J_4$;$^3J_{4ax,10}$) ⌈$^3J_{4eq,10}$⌉*	9,10 δ (spl)[b]	11,11'[a] δ (spl)[b]	13, 13' – 17-17'[a] δ (spl)[b]
11$_{3/3}$	^{1}H	4.75 (t) (4.9)	**ax**: 3.90 (dd) (12.5; 1) **eq**: 4.18 (d)	3.65 (m)	2.7 – 2.9 (br. m)	
(3_3:3)	^{13}C	102.27	69.6	69.4	35.4, 32.9, 32.2, 32.1	
11$_{2/6}$ (6_2:6)	^{1}H	4.74 (t) (5)	**ax**: 3.91 (br. d) (12.5) **eq**: 4.17 (d)	3.65	2.7 – 2.9 (br. m)	
11$_{3/6}$ (6_3:6)	^{1}H	4.75 (t) (5)	**ax**: 3.91 (dd) (12.5; 1) **eq**: 4.18 (d)	3.65	2.7 – 2.9 (br. m)	
	^{13}C	102.2	69.6	69.4	35.5, 32.9, 32.3, 32.2	
15$_{2,3/2}$ ($2_{2,3}$: 2)	^{1}H ^{13}C	4.76 (t) (4.8) 102.3, 102.6	**ax**: 3.90 (br. t) (12.8) **eq**: 4.18 (d) 69.5	3.64, 3.645 69.3	2.7 – 2.9 35.2, 35.0, 32.8, 32.1, 32.0 31.8, 31.5	

[a] The primed atoms are related by C_2 symmetry to the corresponding ones. [b] d = doublet; b = broad; m = multiplet; **eq** = equatorial, **ax** = axial protons.

Table 4. MALDI-TOF mass spectrometric data of ETG$_n$/TOD oligomers and macrocycles.

Molecule	Peaks (rel. int.)	Assignment	Calculated	Molecular formula
Macrocycles				
11$_{3/6}$ (6_3:6)	2343.03 (3)	**11**$_{3/6}$ · K$^+$	2343.3	$C_{84}H_{144}O_{24}S_{24}K$
11$_{2/6}$ (6_2:6)	1983.35 (2)	**11**$_{2/6}$ · K$^+$	1983.3	$C_{76}H_{120}O_{24}S_{18}K$
11$_{3/4}$ (4_3:4)	1575.89 (15) 1559.92 (8)	**11**$_{3/4}$ · K$^+$ **11**$_{3/4}$ · Na$^-$	1575.2 1559.2	$C_{56}H_{96}O_{16}S_{16}K$ $C_{56}H_{96}O_{16}S_{16}Na$
11$_{3/4}$ (4_3:4) with AgTf	1643.72 (35)	**11**$_{3/4}$ · Ag$^+$	1643.1	$C_{56}H_{96}AgO_{16}S_{16}$
11$_{2/4}$ (4_2:4) with AgTf	1403.29 (14)	**11**$_{2/4}$ · Ag$^+$	1403.1	$C_{48}H_{80}AgO_{16}S_{12}$
11$_{3/3}$ (3_3:3)	1175.62 (100)	**11**$_{3/3}$ · Na$^-$	1175.2	$C_{42}H_{72}NaO_{12}S_{12}$
11$_{3/3}$ (3_3:3) with AgTf	1259.91 (93)	**11**$_{3/3}$ · Ag$^+$	1259.1	$C_{42}H_{72}AgO_{12}S_{12}$
11$_{2/3}$ (3_2:3)	995.96 (100) 1011.91 (98)	**11**$_{2/3}$ · Na$^+$ 3+3ETG$_2$K$^+$	995.1 1011.1	$C_{36}H_{60}NaO_{12}S_9$ $C_{36}H_{60}KO_{12}S_9$
Oligomers				
14$_{3/3}$ (3_3:4)	1504.77 (45)	**14**$_{3/3}$ ·Na$^+$	1505.1	$C_{50}H_{84}Br_2NaO_{16}S_{12}$
14$_{3/3}$ (3_3:4) with AgTf	1589.86 (75)	**14**$_{3/3}$ ·Ag$^+$	1589.0	$C_{50}H_{84}AgBr_2O_{16}S_{12}$
14$_{2/3}$ (3_2:4)	1341.73 (4) 1325.73 (4)	**14**$_{2/3}$ · K$^+$ **14**$_{2/3}$ · Na$^+$	1341.1 1325.1	$C_{44}H_{72}Br_2KO_{16}S_9$ $C_{44}H_{72}Br_2NaO_{16}S_9$
14$_{3/2}$ (2_3:3)	1120.95 (100)	**14**$_{3/2}$ · Na$^+$	1121.0	$C_{36}H_{60}Br_2NaO_{12}S_8$
14$_{3/2}$ (2_3:3) with AgTf	1205.90 (100 sat.)	**14**$_{3/2}$ · Ag$^+$	1204.9	$C_{36}H_{60}AgBr_2O_{12}S_8$
14$_{2/2}$ (2_2:3)	1001.82 (22) 1017.80 (17)	**14**$_{2/2}$ ·Na$^+$ **14**$_{2/2}$ ·K$^+$	1001.0 1017.0	$C_{32}H_{52}Br_2NaO_{12}S_6$ $C_{32}H_{52}Br_2KO_{12}S_6$
Molecule	**Peaks (rel. int.)**	**Assignment**	**Calculated**	**Molecular formula**
Macrocycles				
(6_3:6) **11**$_{3/6}$	2343.03 (3) 1959.64 (3) 1574.30 (7) 1190.86 (85)	6:6 · K$^+$ 5:5 · K$^+$ 4:4 · K$^+$ 3:3 · K$^+$	2343.3 1959.3 1575.2 1191.2	$C_{84}H_{144}O_{24}S_{24}K$ $C_{70}H_{120}O_{20}S_{20}K$ $C_{56}H_{96}O_{16}S_{16}K$ $C_{42}H_{72}O_{12}S_{12}K$
(6_2:6) **11**$_{2/6}$	1983.35 (2) 1658.72 (3) 1335.02 (6) 1011.35 (30)	6:6 · K$^+$ 5:5 · K$^+$ 4:4 · K$^+$ 3:3 · K$^+$	1983.3 1659.2 1335.2 1011.1	$C_{76}H_{120}O_{24}S_{18}K$ $C_{60}H_{100}O_{20}S_{15}K$ $C_{48}H_{80}O_{16}S_{12}K$ $C_{36}H_{60}O_{12}S_9K$

Interestingly, with a dithranol matrix, the spectra revealed in addition to the molecular ions, peaks resulting from a peculiar gradual fragmentation of TOD-$CH_2(SCH_2CH_2)_n$ moieties as exemplified for the (6_3:6) $\mathbf{11}_{3/6}$ and (6_2:6) $\mathbf{11}_{2/6}$ at the bottom of Table 4.

Structural Analysis and Computations

X-ray crystallography, see Figures 2, 3, 4, 5, and 6) and molecular modeling, see Figures 7, 8, 9, and 10).

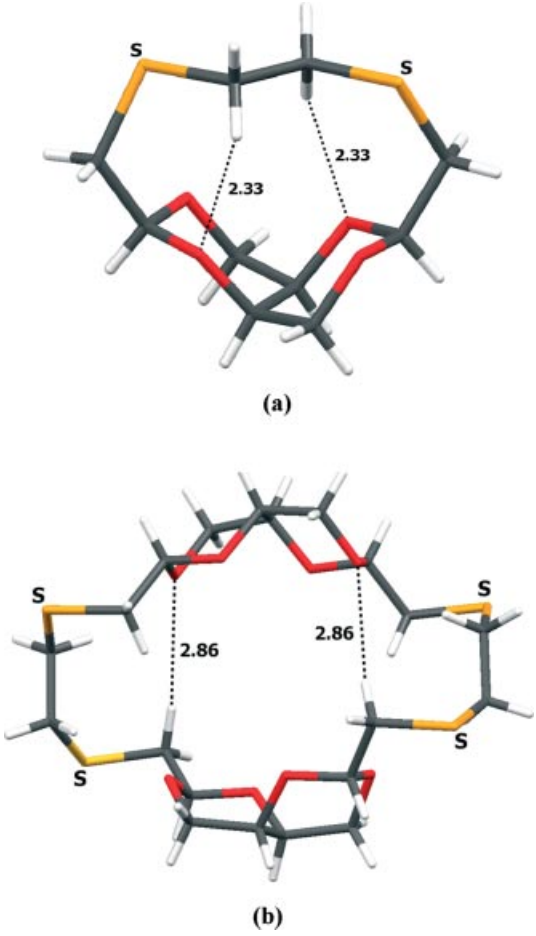

Figure 2. Molecular structures of (a) **7** and (b) **8** (cf. Scheme 4).

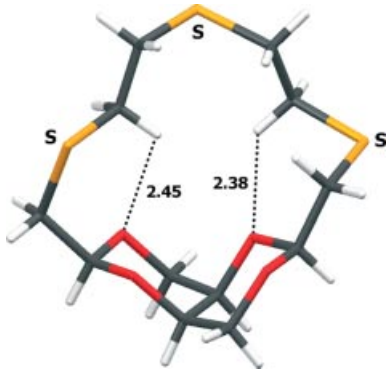

Figure 3. Molecular structure of $\mathbf{7}_2$.

The molecular and crystal structures of *rac*-**7** (space group *Pbcn*) and *rac*-**8** (space group *C*2/*c*), have been included in our preliminary communication,[1g] and are both characterized by a C_2 symmetry, being positioned in the respective crystals on axes of twofold rotation. These pass through, and are aligned perpendicular to, the central C9–C10 bonds of the TOD moieties. Typically, the sulfur atoms along the cyclic framework point outward, and the S–C–C–S moieties reveal an *anti* conformation. This allows to

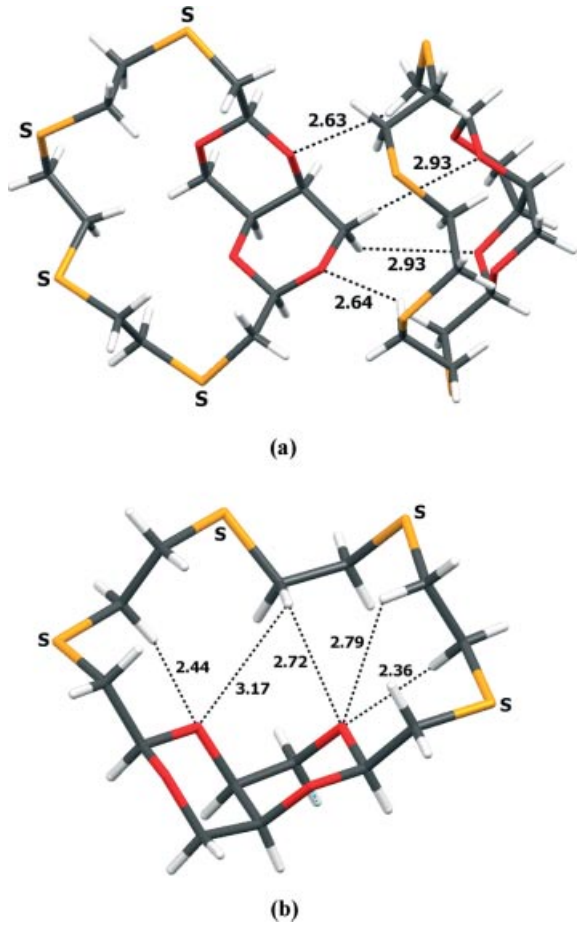

Figure 4. Molecular structure of $\mathbf{7}_3$, showing (a) intramolecular C–H···O interactions and (b) the steric fit and the intermolecular C–H···O attractions between two molecules constituting the asymmetric unit.

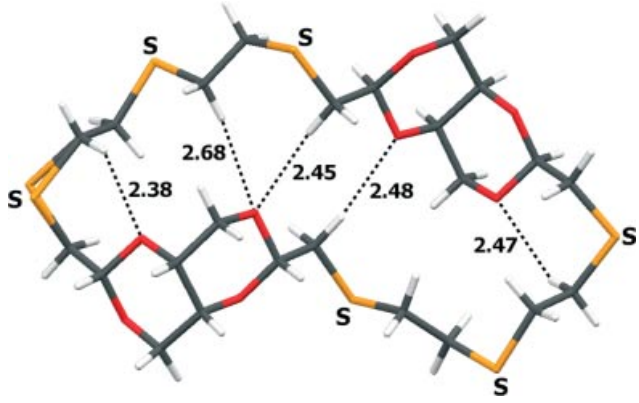

Figure 5. Molecular structure of $\mathbf{8}_2$, showing its squeezed conformation in the crystal.

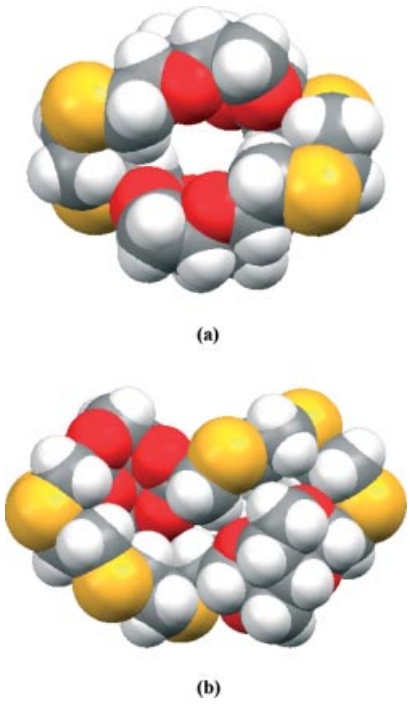

Figure 6. Space-filling illustrations of (a) **8** and (b) $\mathbf{8}_2$.

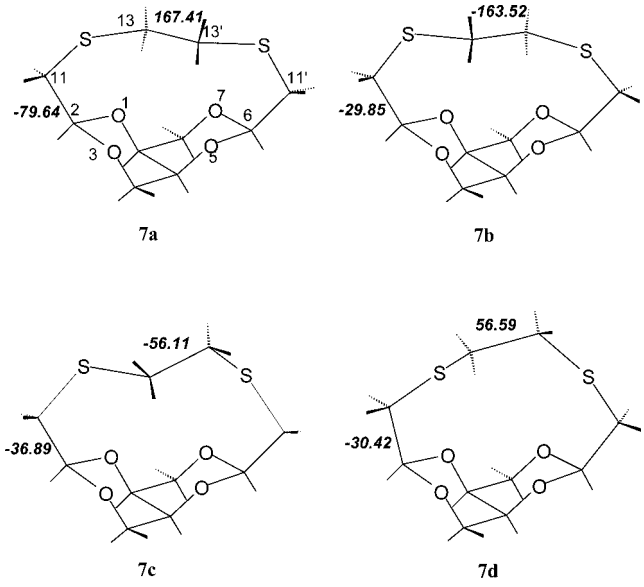

Figure 7. The four stablest conformers of **7** ($E_{rel.}$ = 0.0 kJ/mol for **7a**, 7.2 kJ/mol for **7b**, 2.9 kJ/mol for **7c**, 4.8 kJ/mol for **7d**). Numbers in bold italics are torsion angles.

minimize the repulsive interactions between the O and S atoms, and to stabilize the molecular conformation by the inward-oriented methylene fragments that fill effectively the space within the cyclic framework and exhibiting weak C–H···O contacts (2.33 Å in **7** and 2.86 Å in **8**) across it. This is depicted in Figure 2, showing the conformational features of these compounds that are characterized by the rigid chair-chair conformation of the TOD moieties, outward-turning S atoms, *anti* S–C–C–S torsions, and close CH_2···O contacts. While **7** is intrinsically rigid and even strained,

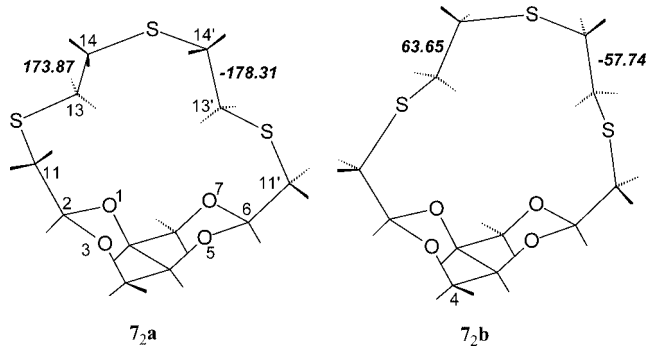

Figure 8. Modelled conformers of $\mathbf{7}_2$; $E_{rel.}$ = 4.8 kJ/mol for $\mathbf{7}_2$**a** and 0.0 kJ/mol for $\mathbf{7}_2$**b**. Numbers in bold italics are torsion angles.

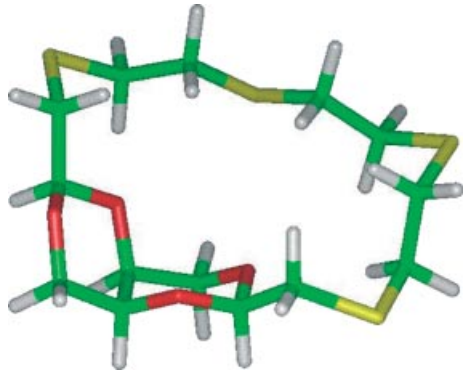

Figure 9. Lowest energy conformer of $\mathbf{7}_3$ from Insight II/AMBER simulated annealing.

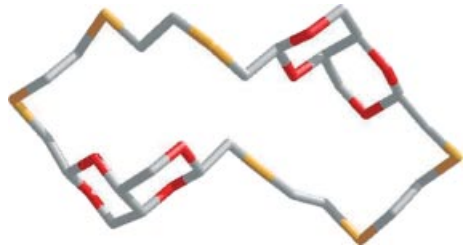

Figure 10. Lowest energy conformer of $\mathbf{8}_2$ from Insight II/AMBER-simulated annealing.

further compression of **8** may be prohibited by the reluctance of the S–C–C–S moiety to deviate significantly from the *anti* geometry.

In order to provide further structural evidence, extended crystallization experiments of other polythiacrown macrocycles were attempted, but X-ray quality crystals of compounds $\mathbf{7}_2$, $\mathbf{7}_3$ and $\mathbf{8}_2$ only could be obtained at this point (for $\mathbf{7}_2$ and $\mathbf{8}_2$ of still rather poor quality).

The 1:1 macrocycle $\mathbf{7}_2$ was obtained from an early reaction mixture starting from racemic (*S*,*S*)-**6**/(*R*,*R*)-**6** (obtained from D,L-threitol), and it crystallized as a racemic material (cf. discussion over Scheme 7). The crystals of the 2:2 analog $\mathbf{8}_2$, however, are enantiomerically pure since they originate from an ulterior set of experiments, starting with L-threitol (Scheme 8). Crystals of $\mathbf{7}_3$ represent also an optically pure material with two independent molecules in the asymmetric unit.

The macrocycle $\mathbf{7}_2$ (Figure 3) adopts a compact conformation in the crystal and its general structural features conform rather well to those of its smaller analog (**7**). Thus, in the aliphatic trithia chain connecting to the two ends of the chair-chair TOD residue all sulfur atoms turn outward, as a result of the typically *anti* S–C–C–S conformation along the chain (with torsion angles of 173° and 174°). Then, however, the adjacent C–S–C–C torsion angles vary between *syn* and *anti*, to allow for a compact conformation that fills effectively the space within the trithia macrocycle. Another noteworthy feature is the short CH_2···O contacts that fill the inner space.

Turning to $\mathbf{7}_3$, however (Figure 4), its most striking feature is that the central S–C–C–S bond is in a *gauche* arrangement, probably due to crystal packing/intermolecular interaction features, since in molecular modeling studies (vide infra), a simulated annealing run for this molecule did not afford the crystallographic structure as the lowest in energy and the lowest energy structure we found (which minimizes intramolecular S···S repulsions) had all *anti* S–C–C–S bonds. In the observed conformation, the tetrathia moiety of the macrocycle extends more parallel to the TOD core rather than perpendicular to it as in $\mathbf{7}_2$, while still maintaining the outward orientation of all four sulfur atoms. This imparts to the $\mathbf{7}_3$ macroring a "bowl' shape, and allows to partly fill its interior by inward-turning C–H groups (Figure 4, a). Noteworthy are the short CH···O interaction distances of 2.36–2.44 Å of both sides of the macrocycle, as in **7** and $\mathbf{7}_2$. These are associated with two wider C–S–C bond angles at both ends of the tetrathia chain (104.3–104.9°) than the C–S–C angles in its central part (99.7–102.1°). The presence of two crystallographically independent molecules (of the same chirality but only slightly different conformation) in the asymmetric unit of this structure can be rationalized by the intermolecular Scheme of the weak C–H···O interactions between them, as well as by effective steric fit of the TOD-edge of one species into the concave surface of the other species (Figure 4, b). In fact, the crystal structure of $\mathbf{7}_3$ can be best described as van der Waals packing such molecular dimers. The cooperative effect of the intra-dimer interactions seems to compensate for the apparent S···S repulsions within the *gauche* SCH_2–CH_2S fragment, wherein the observed distances between the S atoms are 3.561(2) and 3.603(2) Å, somewhat shorter than twice the van der Waals radius of covalently bound sulfur.

Interestingly, it is the above-described conformation-determining features of **7**, $\mathbf{7}_2$, $\mathbf{7}_3$ and **8** which are even more pronounced in crystalline $\mathbf{8}_2$ (Figure 5), and were lagely endorsed by molecular modeling and simulated annealing studies (vide infra). In the large macrocyclic host its observed molecular structure shows a "collapsed" rather than circular conformation, wherein the two TOD fragments do not face one another across the ring as in **8** (see above). Rather, this macrocycle is severely squeezed, in order to place each thrithia chain section over one of the TOD fragments. In the resulting structure, the chain and the fused-ring moieties are in contact. As in the other compounds **7**, **8**, $\mathbf{7}_2$ and $\mathbf{7}_3$ all the S-sites are oriented in the outward direction, and all S–C–C–S torsion angles (with a single exception in $\mathbf{7}_3$) are *anti* (varying within 160–178°). Most of the C–S–C–C torsions, on the other hand, are nearly *syn*/*gauche*, to allow effective closure of the macroring without a significant conformational distortion of the chair-chair TOD fragments. The latter is clearly manifested by the rather short intramolecular CH_2···O distances (of 2.4–2.5 Å) between the contacting fragments (cf. Figure 5). In all these contexts, it is interesting to compare more closely the molecular structures of **8** and $\mathbf{8}_2$.

In **8** (Figure 2 and Figure 6a), the rigidity of the TOD fragments and the short length of the two dithia bridges prevent a more concise conformation of the ring framework without marked and energetically unfavorable deformation of the bond angles therein. Thus, the non-bonding CH_2···O distances across the macrocycle are relatively long (Figure 2), and the inner C–H bonds do not fill completely the void space (ca. 2 Å in diameter) within the ring, as seen in the space-filling model (Figure 6, a).

In $\mathbf{8}_2$, extension of the dithia $–CH_2S(CH_2)_2SCH_2-$ bridges to the longer trithia ensembles $–CH_2S(CH_2)_2S(CH_2)_2-SCH_2-$ provides adequate conformational freedom to afford a folded void free structure (Figure 5 and Figure 6b). One can see there the conformational disorder associated with the leftmost sulfur, the *anti* conformation about all the S–C–C–S bonds, as well as the short CH_2···O contacts that fill the inner space. Note also that all the S atoms point outward and, as opposed to the open ring structure and lack of close C–H···O contacts in (a), the folded self-filled molecular structure in (b) enables more effective C–H···O bonds/interactions.

All four structures reveal a considerable shortening of the carbon-carbon bonds in the S–C–C–S fragments (with

Table 5. Selected structural parameters of the S-containing chains.

Compound	**7**[e]	**8**[e]	$\mathbf{7}_2$	$\mathbf{7}_3$[e]	$\mathbf{8}_2$
SC–CS[a]	1.497	1.525	1.423–1.485	1.514–1.522	1.477–1.514
$[SC–CS]_{average}$	1.497	1.525	1.454	1.519	1.494
S–C[a]	1.801–1.827	1.796–1.808	1.799–1.866	1.805–1.821	1.789–1.884
C–S–C[b]	104.7	100.7–101.0	100.6–101.9	99.7–104.9	100.5–104.5
S–C–C–S[d]	178.0	157.0	173.4–173.7	174.7–179.7	160.3–178.0
$[S–C–C–S]_{average}$	178.0	157.0	173.6	177.2 68.5, 74.7[f]	170.5

[a] Bond length range [Å]. [b] Bond angle range [°]. [d] Torsion angle range *anti* [°]. [e] Structures determined with higher precision. [f] *syn* torsion angles.

one exception), as compared to standard C(sp^3)–C(sp^3) values, analogous to that observed in the OC–CO bonds in crown ethers (irrespective of whether the conformation about these bonds is *syn* or *anti*). Selected covalent param-

Table 6. Selected bond lengths [Å], bond angles [°] and torsion angles [°] for **7**, $\mathbf{7}_2$, $\mathbf{7}_3$ and **8**, according to the atom numbering illustrated in the adjacent $\mathbf{7}_3$ structure.

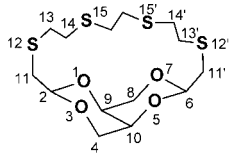

Parameter ⇓ Cpd. ⇒	7	7_2	7_3	8	8_2
Bond lengths					
O1–C2 O5–C6 / O1a–C2a	1.420	1.403 1.393	1.415, 1.416 1.415, 1.421	1.398 1.401	1.409, 1.413 1.412, 1.412
O1–C9 O5–C10 / O1a–C9a	1.426	1.449 1.478	1.433, 1.443 1.437, 1.441	1.456 1.434	1.432, 1.433 1.437, 1.441
O3–C2 O7–C6 / O3a–C2a	1.399	1.428 1.410	1.416, 1.419 1.411, 1.415	1.406 1.406	1.409, 1.413 1.395, 1.412
C2–C11 C6–C11' / C2a–C11a	1.512	1.515 1.534	1.507, 1.514 1.505, 1.512	1.500 1.513	1.504, 1.516 1.498, 1.515
O3–C4 O7–C8 / O3a–C4a	1.423	1.435 1.455	1.430, 1.440 1.429, 1.434	1.422 1.438	1.429, 1.441 1.418, 1.442
C4–C10 C8–C9 / C4a–C10a	1.512	1.477 1.498	1.504, 1.507 1.506, 1.510	1.494 1.495	1.491, 1.507 1.497, 1.506
C9–C10 C9a–C10a	1.523	1.509	1.527, 1.527	1.491 1.517	1.533 1.499
C11–S12 C11'–S12' / C11a–S12a	1.801	1.820 1.819	1.805, 1.814 1.807, 1.808	1.807 1.793	1.805, 1.809 1.789, 1.800
S12–C13 S12'–C13' / S12a–C13a	1.827	1.870 1.838	1.817, 1.818 1.817, 1.818	1.808 1.795	1.812, 1.856 1.827, 1.866
C13–C13' C13–C13a	1.497			 1.527	
C13–C14 C13'–C14'		1.514 1.434	1.514, 1.518 1.518, 1.519		1.484, 1.514 1.477, 1.503
C14–S15 C14'–S15		1.829 1.814	1.814, 1.817 1.817, 1.819		1.817, 1.822 1.799, 1.865
Bond angles					
C2–O1–C9 C6–O5–C10 / C2a–O1a–C9a	115.0	113.0 111.4	110.6, 112.2 111.3, 111.4	111.1 111.5	111.8, 112.4 111.5, 111.5
C2–O3–C4 C6–O7–C8 / C2a–O3a–C4a	112.5	112.0 112.4	110.7, 111.2 110.8, 111.6	112.1 111.4	111.2, 111.6 110.8, 112.8
O3–C4–C10 O7–C8–C9 / O3a–C4a–C10a	110.3	111.9 109.4	110.1, 111.5 110.8, 111.6	111.4 110.7	110.8, 111.5 110.2, 111.0
O1–C9–C8 O5–C10–C4 / O1a–C9a–C8a	106.8	107.5 107.6	108.0, 108.6 107.9, 108.6	107.6 108.3	108.1, 108.8 108.2, 108.2
Torsion angles					
C2–O1–C9–C10 C6–O5–C10–C9 / C2a–O1a–C9a–C10a	–51.1	–57.0 –52.5	–54.1, –57.8 –55.6, –56.7	–54.8 –53.2	–53.7, –55.1 –53.9, –56.5
C2–O1–C9–C8 C6–O5–C10–C4 / C2a–O1a–C9a–C8a	–170.2	–177.3 –174.6	–177.3, –174.0 –175.4, –177.0	–177.8 –174.9	–174.9, –176.6 –176.1, –177.8
O1–C9–C8–O7 O3–C4–C10–O5 / O1a–C9a–C8a–O7a	66.4	66.8 70.2	68.3, 70.3 67.8, 70.4	75.8 78.1	70.6, 72.4 68.9, 72.7
H2–C2–C11–H11A H6–C6–C11'–H11'A / H2a–C2a–C11a–H11aA	39.3	54.7 –45.6	–171.7, –171.9 176.6, 177.7	169.6 169.2	–168.7, –178.6 –176.0, –177.0
H2–C2–C11–H11B H6–C6–C11'–H11'B/H2a–C2a–C11a–H11aB	–76.3	170.8 70.1	71.8, 72.1 –65.9, –67.0	–73.6 –73.6	66.6, 75.0 –62.4, –63.2

eters relevant to the present crystallographic data are summarized in Table 5.

One additional feature worth pointing out is the significant deformation of the TOD core in the structure of **7** (Table 6), relative to the larger macrocycles $\mathbf{7}_n$, **8** and $\mathbf{8}_2$, as well as to open TOD systems, the structures of which were reported in previous studies,[1c,1h] apparently due to restricted rotation about the bonds in the strained bridge of **7**.

Molecular modeling probes were in order and we performed conformational searches for some of the these molecules, using the molecular dynamics/energy minimization protocol implemented in INSIGHTII's DISCOVER module and the AMBER forcefield. Thus, for **7**, at 500 °C during 800 ps with geometry optimization every 10 ps, we ended up with six forms, the four lowest ones shown in Figure 7. The most stable one **7a**, is indeed very similar to the experimental, X-ray crystal structure analysis result (vide supra), as expected of this relatively inflexible molecule.

While the two less stable conformers (**7c** and **7d**) exhibit contorted S–CH_2–CH_2–S *gauche* forms, the C_2 symmetric **7a**, as well as **7b**, possess *anti* S–CH_2–CH_2–S bridges. Interestingly, what appears to make **7a** more stable than **7b**, is the arrangement enabling C–H···O double hydrogen bonding to the central O–C–C–O moiety, seconding the X-ray findings (Figure 2).

All this points to **7** adopting the same conformations in (chloroform) solution as in the crystal (for example, the O1–C2–C11–S12/O5–C6–C11′–S12' torsion angles amount to ca. 30°.) and fits, in fact, the ^{1}H NMR spectrum of **7** (as opposed to the larger ring in the series - cf. Table 3 below), having the respective H2 signal not only shifted to lower field, but changed from triplet to doublet, corresponding with the above torsion angles (Table 3).

To be sure, the X-ray structures of **7** (and analogues) is well reproduced not only by AMBER, but also by MM3 calculations, except for the bridge S–C–C–S bond shortening. The short SC–CS bonds in thiacrown ethers are documented in the literature,[13] as is that of OC–CO bonds in crowns, and we have also encountered and discussed this phenomenon.[1k]

Both NMR (Table 3) and X-ray analysis (Table 5) indicate that structure $\mathbf{7}_2$ is not strained. AMBER conformational search for $\mathbf{7}_2$ at the 300, 400 and 500 °C reveals in the range of 6 kJ/mol a number of conformations (none of them being symmetrical!) with *gauche*/*gauche, gauche*/*anti* and *anti*/*anti* S–CH_2–CH_2–S units in the bridge. One of the *anti*/*anti* conformers ($\mathbf{7}_2$**a** in Figure 8) is very close to the X-ray structure of $\mathbf{7}_2$, but the lowest energy form is the *gauche*/*gauche* conformer $\mathbf{7}_2$**b**.

In the same context and behaviour, simulated annealing of $\mathbf{7}_3$ did not afford either the crystallographic structure as the most stable one, in all probability due to the intermolecular interactions in the crystal (Figure 4), and its lowest energy structure (Figure 9) exhibits an all *anti* S–C–C–S bridge.

As to the 2:2 macrocycle **8**, conformational search (AMBER) at 300, 400 and 500 °C reveals several stable conformations with *gauche*/*gauche*, *gauche*/*anti* and *anti*/*anti* S–CH_2–CH_2–S units in the bridge, in the short range of about 3 kJ/mol. Some of the *anti*/*anti* forms have C_2 symmetry, but neither of them resembles the crystal structure of **8** (Figure 9, b),[1g] with only small differences in parameters (Table 5) of the two TOD units in **8** precluding high symmetry (D_2) of the macrocycle. In fact, geometry optimization using the crystal coordinates resulted in a perfect *anti*/*anti* conformer and D_2 symmetry, the energy of which was more than 20 kJ/mol higher than the average value resulting from conformational search. While such differences in $\mathbf{7}_2$, $\mathbf{7}_3$ and **8** suggest that packing forces play a major role in differentiating the crystallographic vs. molecular conformational behaviour of these macrocycles, it was refreshing to establish that simulated annealing (Insight II) of the 2:2 macrocycle $\mathbf{8}_2$ provides a lowest energy structure (Figure 10), similar to the X-ray crystallographic one (Figure 5) barring the local conformational disorder within.

Concluding Remarks

We put forward a unique class of polythiacrown macro-, giganto- and ultracyclic systems, consisting of ethylene 1,2-dithioglycol (ETG) to poly(ethylene thioglycol) (ETG_n) bridges over one to six *cis*-1,3,5,7-tetraoxadecalin (TOD) diacetal units, having ETG_n/TOD ratios of 1:1 (**7**), 2:2 (**8**), 3:3 ($\mathbf{11}_{n/3}$), 4:4 ($\mathbf{11}_{n/4}$) and 6:6 ($\mathbf{11}_{n/6}$), as well as the intermediate 1:2 ($\mathbf{14}_{n/1}$), 2:3 ($\mathbf{14}_{n/2}$) and 3:4 ($\mathbf{14}_{n/3}$) oligomers. Both stochastic and controlled approaches were taken to prepare these systems and detailed NMR and MS spectroscopy, X-ray crystallographic analysis and MM and MD computations were performed, to construct a coherent picture of their structure, stereochemistry and remarkable interrelationship. The length and complexity of this report prohibit inclusion of available metal-ion complexation data, which will be presented in a separate publication.

Experimental Section

General: All reactions were carried out in commercially pure or purified dry solvents under argon (Ar) and monitored by TLC and/or by ^{1}H NMR spectroscopy. Column chromatography was performed on Merck silica gel (60, 0.040–0.063 mm) unless indicated otherwise. Melting points were determined on a Büchi capillary melting point apparatus and are not corrected. ^{1}H and ^{13}C NMR spectra were recorded routinely on AC-200 and ARX-400 or -500 Bruker spectrometer in $CDCl_3$. All chemical shifts are δ-values in ppm: for ^{1}H relative to TMS as internal standard and for ^{13}C relative to $CDCl_3$ (center of triplet 77 ppm) – except for spectra in CD_3CN which are relative to CD_3CN (center of heptet δ = 0.2 ppm). The results are collectively tabulated in Table 2 and Table 3. Mass spectra (EI-MS, CI-MS and FAB) were recorded on a VG Autospec 250 mass spectrometer and high resolution mass spectrometric (HRMS) data were obtained for all new compounds. MALDI-TOF MS analyses were performed on a Reflex IV Bruker Daltonics instrument and the results are tabulated in Table 4. The smaller compounds could be measured even without any matrix but regularly we used as matrix DHB in THF. Dithranol (1,8,9-trihydroxyanthracene) in chloroform was also used, but a peculiar

gradual fragmentation of TOD–$CH_2(SCH_2CH_2)_n$ moieties was observed. This behaviour was observed in all measured spectra using dithranol matrix and is worth noting for any other polythiamacrocycles under potential scrutiny. IR spectra were recorded with a Nicolet 205 FTIR instrument in KBr pellets. The dithiols used were commercial or self produced[16] materials, except 3,6-dithiaoctane-1,8-dithiol, which was prepared as described.[17] (*S*,*S*)-2,6-bis(bromomethyl)-1,3,5,7-*cis*-TOD (**6**),[1k] $[\alpha]_D$ = 30.80 was prepared from L-threitol $[\alpha]_D$ = 13.42, and similarly the racemates. Selected optical rotation measurements were at 20 °C.

Abbreviations: DHB = 2,5-dihydroxybenzoic acid, TOD = 1,3,5,7-*cis*-tetraoxadecalin.

2,6-Bis(phenylthiomethyl)-TOD (5, R = CH_2SPh): Sodium (0.1 g, 4.3 mmol) was added to absolute ethanol (4 mL) and, after complete dissolution, thiophenol (0.38 g, 3.4 mmol) was added followed by **6** (0.33 g, 1 mmol). The mixture was stirred at 55 °C for 4 h after which 20 mL of water was added. The precipitated product was filtered off, washed with 20 mL of water and 3 mL of methanol and dried. Yield 380 mg, 97%, m.p. 125–127 °C. HR-MS (70 eV): *m*/*z* 390.0964 (M^+, calcd. for $C_{20}H_{22}O_4S_2$ 390.0960).

General Procedure for the Preparing of Macrocycles from ETG_n and 2,6-Bis(bromomethyl)-TOD (6) (see Schemes 4 and 5): ETG_n (2 mmol) and Cs_2CO_3 (2 g, 6 mmol) were added to 150 mL of CH_3CN and the mixture was brought to reflux under Ar. To this well-stirred and refluxing mixture, a solution of **6** (665 mg, 2 mmol) in 5 mL of CH_3CN was added and the reaction mixture was refluxed for 3 h. After cooling and filtering, the solution was evaporated and the crude product was resolved by chromatography as indicated. Observed but unisolated products were identified by mass spectrometry. Products for X-ray analysis were crystallized usually from isopropyl alcohol.

Reaction of 6 with ETG (see Scheme 5): The reaction of *rac*-**6** with ETG (**12**) under the conditions described above provided a crude product that was chomatographed on neutral alumina (containing 3% water) and eluted with diethyl ether. The order of elution was: a mixture of ETG_ns (17 mg),[16] **6** (20 mg, 3%), **7** (105 mg, 20%), byproduct $\mathbf{7}_2$ (7 mg, 1%), and a mixture of *rac*- and *meso*-**8** (23 mg, 4%). The same reaction in DMF provided negligible yields of those products along with **10** and the spurious compound **X** (see below).

The above reaction was carried out also at room temperature for 55 h and the crude product was separated on silica gel (elution gradient: chloroform; chloroform/ethyl acetate; ethyl acetate; ethyl acetate/acetone), the products were obtained in the following order: a mixture of dithiols (4 mg), **7** (15 mg, 3%), **10** (10 mg, 1.5%), *meso*-**8** (23 mg, 4.4%), *rac*-**8** (26 mg, 4.9%), *rac*-$\mathbf{11}_{1/3}$ (3_1:3) (22 mg, 4.1%), *rac*-$\mathbf{11}_{1/4}$ (4_1:4) (33.5 mg, 6.0%), [(6_1:6) ($\mathbf{11}_{1/6}$) with a trace of (5_1:5) ($\mathbf{11}_{1/4}$) (11.5 mg, 1.8%)] – identified mass spectrometrically – and finally a mixture of ill-defined polymeric material (38.5 mg).

2,6-(2′,5′-Dithiahexano-1′,6′)-TOD (7): M.p. 166–168 °C. HR-MS (70 eV): *m*/*z* 264.0491 (M^+, calcd. for $C_{10}H_{16}O_4S_2$ 264.0490).

2,6a:6,2a-Bis(2′,5′-dithiahexano-1′,6′)-bis(TOD) (8): M.p. 224–225 °C. HR-MS (70 eV): *m*/*z* 528.0951 (M^+, calcd. for $C_{20}H_{32}O_8S_4$: 528.0980).

2,6-(2′,5′,6′,9′-Tetrathiadecano-1′,10′)-TOD (10): M.p. 161–162 °C. HR-MS (70 eV): *m*/*z* 356.0239 (M^+, calcd. for $C_{12}H_{20}O_4S_4$ 356.0244).

Reaction of 6 with ETG_2: Using the above described general procedure, the reaction of **6** (665 mg, 2 mmol) with the dithiol $\mathbf{12}_2$ (355 mg, 2.07 mmol) provided a crude product which was chromatographed (neutral alumina + 3% water, eluent diethyl ether), to provide starting ETGs and **6** (ca. 2%) followed by $\mathbf{7}_2$ (220 mg, 34%).

2,6-(2′,5′,8′-Trithianonano-1′,9′)-TOD ($\mathbf{7}_2$): M.p. 169–170 °C. HR-MS (70 eV): *m*/*z* 324.0514 (M^+, calcd. for $C_{12}H_{20}O_4S_3$ 324.0524).

Reaction of 6 with ETG_3: The general procedure was followed, using **6** and the dithiol $\mathbf{12}_3$ (450 mg, 2.10 mmol). The crude product was chromatographed (neutral alumina + 3% water, eluent diethyl ether), providing a small amount of starting materials, ETGs and **6**, followed by $\mathbf{7}_3$ (350 mg, 46%).

2,6-(2′,5′,8′,11′-Tetrathiadodecano-1′,12′)-TOD ($\mathbf{7}_3$): M.p. 179–180 °C, $[\alpha]_D$ = 13.84, HR-MS (70 eV): *m*/*z* 384.0580 (M^+, calcd. for $C_{14}H_{24}O_4S_4$ 384.0558).

Targeted Preparation of X and 10: A solution of **6** (332 mg, 1 mmol), ETG (**12**) (1 mL, 12 mmol) and triethylamine (1 mL, 7 mmol) in DMF (12 mL) was stirred overnight at 100 °C. After evaporation of the DMF, the solid residue was washed twice with 20 mL of chloroform, to provide the product **X** (215 mg), which is insoluble in chloroform (and very soluble in water). The unified chloroform washings were evaporated and the residue was chromatographed (neutral alumina + 3% water) to provide (elution with diethyl ether) crystals of the disulfide **10** (12 mg) (vide supra).

2,6-Bis(dimethyliminiomethoxymethyl)-TOD Dibromide (X): IR (KBr): 978, 996, 1020, 1045, 1060, 1084, 1137, 1156, 1178, 1253, 1364, 1384, 1452, 1473, 1656 (m), 2713, 2796, 2811, 2871, 2919, 2977, 3000, 3400 cm^{-1} (br). ^1H NMR (D_2O, δ, ppm): 2.95 (s, 12 H, CH_3), 3.39 (d, $^3J_{H11,H2}$ = 4.3 Hz, 4 H, H11), 4.0 (m, 6 H, H4 and H9), 5.23 (dd, 2 H, H2). MS-CI: 261 ($C_{11}H_{19}O_6N^+$), 341, 343.

Reaction of 6 with 2,6-Bis(2-thiabutane-4-thiol)-TOD (9) (see Scheme 6): To a stirred, ice-cooled mixture of (9*S*,10*S*)-**6** (332 mg, 1 mmol) and Cs_2CO_3 (3 g, 9 mmol) in 20 mL of acetonitrile (under Ar), ETG (2 g, 21 mmol) was added and stirring was continued while room temperature was reached overnight. The reaction mixture was filtered (under Ar) and the solvents were evaporated in vacuo. The residue was washed (under Ar) with 100 mL PE and dissolved in 20 mL of acetonitrile (Solution 1). To a stirred, refluxing (under Ar) solution of (9*S*,10*S*)-**6** (332 mg, 1 mmol) and Cs_2CO_3 (3 g, 9 mmol) in 100 mL of acetonitrile, "Solution 1" (containing mostly **9**) was added with strict exclusion of air and reflux/stirring was continued (under Ar) during 1 h. After cooling, filtration and evaporation, the crude product was separated on silica gel. Elution with gradient PE/ethyl acetate provided first some polyethylene dithiols (2.5 mg), followed by **6** (16 mg, 2.5%), **8** (100 mg, 19%), and minute amounts of $\mathbf{11}_{1/3}$ and of a mixture of oligomeric material ($\mathbf{13}_{1/m}$).

General Procedure for Oligomers ($\mathbf{14}_{n/m}$) (see Schemes 8 and 9): ETG_n (0.37 mmol), 2,6-bis(bromomethyl)-TOD (**6**) (1 mmol) and K_2CO_3 (250 mg) were suspended in 20 mL of oxygen-free acetonitrile (Ar-saturated for 30 min) and refluxed under Ar for 6 h. The mixture was filtered, washed with acetonitrile and the solid residues were triturated with CH_2Cl_2 and $CHCl_3$. The combined filtrates were evaporated and the residues chromatographed (alumina type II, elution with PE/CH_2Cl_2 in decreasing ratio). Typical yields (of isolated pure compounds) from the reaction of **6** (3.88 g, 11.7 mmol) with $\mathbf{12}_2$ (0.920 g, 4.3 mmol) were: starting material **6** (1.5 g, 38%), oligomer ($\mathbf{14}_{3/1}$) (765 mg, 24.9%), macrocycle ($\mathbf{7}_3$) (26 mg, 1.7%), oligomer ($\mathbf{14}_{3/2}$) (415 mg, 17.6%), oligomer ($\mathbf{14}_{3/3}$) (100 mg, 4.7%).

2,6a-Bis(bromomethyl)-6,2a-(2′,5′,8′,11′-tetrathiadodecano-1′,12′)-bis(TOD) ($\mathbf{14}_{3/1}$): MS-CI 715.0 [MH^+], $[\alpha]_D$ = 5.65.

2,6b-Bis(bromomethyl)-6,2a;6a,2b-bis(2′,5′,8′,11′-tetrathiadodecano-1′,12′)-tris(TOD) ($14_{3/2}$): MS-FAB 1098.7 [MH^+].

2,6c-Bis(bromomethyl)-6,2a;6a,2b;6b,2c-tris(2′,5′,8′,11′-tetrathiadodecano-1′,12′)-tetrakis(TOD) ($14_{3/3}$): See Tables 2 and 4.

General Procedure for the Preparation of 1:1, 2:2 and 3:3 ETG_n/TOD Macrocycles (7_n, 8_n, $11_{n/3}$) from TOD (6) or $14_{n/m}$[10] and ETG_n (12_n) (see Schemes 4, 10 and 11): ETG_n (1.5 mmol), TOD-dibromide (**6**) (1.5 mmol) and K_2CO_3 (1.4 g) were suspended in oxygen-free (Ar-saturated for 30 min) acetonitrile (100 mL), vigorously stirred and refluxed under Ar for 6 h. The reaction was filtered while hot, washed with dichloromethane. The combined filtrates are evaporated and chromatographed on alumina (type II, PE/CH_2Cl_2 in increasing polarity), to afford the smaller macrocyles (up to 3:3). Typically, the reaction of **6** (0.485 g, 1.46 mmol) with ETG_3 (12_3) (0.313 g, 1.46 mmol) and K_2CO_3 (1.4 g) provided: starting material **6** (150 mg, 35%), 7_3 (183 mg, 37%), [by-products (7_4) (10 mg, 2%, due to the presence of 12_4 impurity in the starting dithiol) and ETG_3-disulfide (10_3) (13 mg, 1.7%)] and 8_3 (28 mg, 5.1%).

2,6-(2′,5′,8′,11′,14′-Pentathiapentadecano-1′,15′)-TOD (7_4): MS (EI-HR): 444.0619 (M^+), calcd. 444.0591 ($C_{16}H_{28}O_4S_5$).

2,6-(2′,5′,8′,11′,12′,15′,18′,21′-Octathiaeicosaduano-1′,22′)-TOD (10_3): MS (CI) 597.1 [MH^+].

2,6a:6,2a-Bis(2′,5′,8′,11′-tetrathiadodecano-1′,12′)-bis(9*S*,10*S*)-TOD (8_3): MS(CI) 769.1[MH^+].

Analogously, **6** and ETG_2 afforded 7_2 (53%) and 8_2 (5%), along with the corresponding accompanying products.

2,6a:6,2a-Bis(2′,5′,8′-trithianonano-1′,9′)-bis(9*S*,10*S*)-TOD (8_2): EI-MS 648.3 (M^+).

General Procedure for the Preparation of Large TOD-Thiamacrocycles $11_{n/m}$[10] (see Schemes 10 and 11): ETG_n (0.5 mmol), dibromo oligomer (0.5 mmol) and K_2CO_3 (1 g) are suspended in oxygen-free acetonitrile (20 mL, Ar-saturated for 30 min) and refluxed under Ar for 6 h. The mixture was cooled to room temperature, filtered and the solids washed with cold acetonitrile. Trituration with CH_2Cl_2 and $CHCl_3$ afforded the large-sized macrocycles. The acetonitrile filtrates were evaporated and the residues chromatographed on alumina (type II); eluted (PE/CH_2Cl_2 in decreasing ratio) to afford the desired macrocyles.

Typical yields for the reaction products from $14_{3/1}$ (0.340 g, 0.47 mmol) with 12_3 (0.110 g, 0.51 mmol): gigantocycle $11_{3/4}$ (150 mg, 41%), macrocycle 8_3 (35 mg, 19%) and traces of macrocycle 7_3 and of starting oligomer $14_{3/1}$.

Typical yields for the reaction products (in order of isolation) from $14_{3/2}$ (0.220 g, 0.20 mmol) with 12_3 (0.050 g, 0.23 mmol): ultracycle $11_{3/6}$ (115 mg, 50%), macrocycles 7_3 (2 mg, 2.5%) and 8_3 (8 mg, 5.2%), starting oligomer $14_{3/2}$ (5 mg, 2.3%) and macrocycle $11_{3/3}$ (13 mg, 5.6%) and some undefined oligo- and polymeric material.

X-ray Diffraction Analyses

2,6a;2a,6b;2b,6-Tris(2′,5′,8′,11′-tetrathiadodecano-1′,12′)-tris(TOD) ($11_{3/3}$) and 2,6a;2a,6b;2b,6c;2c,6d;2d,6e;2e,6-Hexakis(2′,5′,8′,11′-tetrathiadodecano-1′,12′)-hexakis(TOD) ($11_{3/6}$): The measurements were carried out with Mo-K_α radiation, on Nonius-CAD4 (for 7_2) and Nonius KappaCCD (for 7_3 and 8_2) diffractometers. Diffraction experiments were conducted at room temperature (ca. 293 K) for 7_2, and at ca. 110 K for 7_3 and 8_2 in order to optimize the quality of the structural results, and in the latter case also to minimize the conformational disorder 8_2 exhibits (see below). Crystals of 7_2 and 8_2 diffracted poorly, which limited somewhat the precision of the structural determination; those of 7_3 appeared much more robust and their analysis yielded more accurate results.

Crystal Data of 7_2: $C_{12}H_{20}O_4S_3$, M = 324.46, monoclinic, space group $P2_1/n$, a = 9.225(2), b = 13.148(4), c = 12.828(5) Å, β = 105.46(2)°, V = 1499.6(8) Å^3, Z = 4, T = 293(2) K, D_c = 1.437 g cm^{-3}, μ(Mo-K_α) = 0.50 mm^{-1}, 1796 unique reflections to $2\theta_{max}$ = 46.0°, 172 refined parameters, R_1 = 0.079 for 1233 observations with $I > 2\sigma(I)$, R_1 = 0.115 (wR_2 = 0.194) for all unique data, $|\Delta\rho|_{max}$ = 0.46 e/Å^3.

7_3: $C_{14}H_{24}O_4S_4$, M = 384.57, orthorhombic, space group $P2_12_12_1$, a = 8.7849(1), b = 19.1743(2), c = 20.9126(3) Å, V = 3522.61(7) Å^3, Z = 8, T = 110(2) K, D_c = 1.450 g cm^{-3}, μ(Mo-K_α) = 0.55 mm^{-1}, 7670 unique reflections to $2\theta_{max}$ = 54.2°, 398 refined parameters, R_1 = 0.034 for 6575 observations with $I > 2\sigma(I)$, R_1 = 0.047 (wR_2 = 0.082) for all unique data, $|\Delta\rho|_{max}$ = 0.45 e/Å^3.

8_2: $C_{24}H_{40}O_8S_6$, M = 648.92, monoclinic, space group $P2_1$, a = 5.3950(1), b = 15.6509(4), c = 18.4342(6) Å, β = 98.284(1)°, V = 1540.28(7) Å^3, Z = 2, T = 110(2) K, D_c = 1.399 g cm^{-3}, μ(Mo-K_α) = 0.48 mm^{-1}, 3470 unique reflections to $2\theta_{max}$ = 55.7°, 361 refined parameters, R_1 = 0.046 for 3171 observations with $I > 2\sigma(I)$, R_1 = 0.052 (wR_2 = 0.125) for all unique data, $|\Delta\rho|_{max}$ = 0.57 e/Å^3. The molecular conformation is characterized by partial disorder with one of the S atoms adopting two equally populated sites. This apparent disorder affects the accuracy of the observed covalent parameters in the close vicinity of this atom.

CCDC-292079 (for 7_2), -292080 (for 7_3) and -292081 (for 8_2) contain the supplementary crystallographic data for this paper. These data can be obtained free of charge from The Cambridge Crystallographic Data Centre via www.ccdc.cam.ac.uk/data_request/cif.

Molecular Modeling: Molecular modeling was carried out with the BIOSYM 1998 package, using *InsightII*.[15] The *Builder* module was used for starting structures for conformational search, *Discover* for molecular dynamics and energy minimizations and *Analysis* for constructing and analysing conformer energy and geometry trajectories. The AMBER force field (within *Insight II*) reproduced best most of the crystal structures of the molecules under study. Conformational searches were done using Molecular Dynamics (MD)/Energy Minimization (EM) technique which consists of constant temperature MD simulation for the molecule with dynamic structure sampling and energy minimization at defined time intervals, conducing to a set of lowest-energy conformers.

Acknowledgments

We gratefully acknowledge support by research grants from the Israel Science Foundation, the Ministry of Science and an Intel Award (to N.G.L.), as well as the valuable assistance of Mr. Shimon Hauptman with mass spectrometry and of Ms. Zafra Stein with X-ray crystallography.

[1] a) H. Senderowitz, A. Linden, L. Golender, S. Abramson, B. Fuchs, *Tetrahedron* **1994**, *50*, 9691 ; b) H. Senderowitz, L. Golender, B. Fuchs, *Tetrahedron* **1994**, *50*, 9707; c) S. Abramson, E. Ashkenazi, M. Greenwald, S. Weinman, I. Goldberg, B. Fuchs, *J. Chem. Soc., Chem. Commun.* **1994**, 1611; d) K. Frische, M. Greenwald, E. Ashkenasi, N. G. Lemcoff, S. Abramson, L. Golender, B. Fuchs, *Tetrahedron Lett.* **1995**, *36*, 9193; e) L. Golender, H. Senderowitz, B. Fuchs, *J. Mol. Struct. THEOCHEM* **1996**, *370*, 221; f) H. Jatzke, K. Frische, M. Greenwald, L. Golender, B. Fuchs, *Tetrahedron* **1997**, *53*, 4821; g) M. Grabarnik, I. Goldberg, B. Fuchs, *J. Chem. Soc., P1* **1997**, 3123; h) A. Linden, C. Rüchardt, H.-D. Beckhaus, S. P.

Verevkin, B. Ganguly, B. Fuchs, *J. Org. Chem.* **1998**, *63*, 8205; i) B. Ganguly, B. Fuchs, *J. Org. Chem.* **2000**, *65*, 558; j) M. Grabarnik, S. Abramson, N. G. Lemcoff, R. Madar, S. Weinman, B. Fuchs, *J. Org. Chem.* **2000**, *65*, 1636; k) S. Abramson, E. Ashkenazi, K. Frische, I. Goldberg, L. Golender, M. Greenwald, N. G. Lemcoff, R. Madar, S. Weinman, B. Fuchs, *Chem. Eur. J.* **2003**, *9*, 6071; l) B. Fuchs, A. Nelson, A. Star, J. F. Stoddart, S. Vidal, *Angew. Chem.* **2003**, *115*, 4352; *Angew. Chem. Int. Ed.* **2003**, *42*, 4220.

[2] a) O. Reani, M. Grabarnik, I. Goldberg, S. Abramson, A. Star, B. Fuchs, *Tetrahedron Lett.* **1997**, *38*, 8073; b) O. Reany, I. Goldberg, S. Abramson, L. Golender, B. Ganguly, B. Fuchs, *J. Org. Chem.* **1998**, *63*, 8850.

[3] a) A. Star, N. G. Lemcoff, I. Goldberg, B. Fuchs, *Tetrahedron Lett.* **1997**, *38*, 3573; b) A. Star, B. Fuchs, *J. Org. Chem.* **1999**, *64*, 1166; c) A. Star, I. Goldberg, N. G. Lemcoff, B. Fuchs, *Eur. J. Org. Chem.* **1999**, 2033; d) A. Star, I. Goldberg, B. Fuchs, *Angew. Chem.* **2000**, *112*, 2797; *Angew. Chem. Int. Ed. Angew. Chem. Int. Ed. Engl.* **2000**, *39*, 2685; e) A. Star, I. Goldberg, B. Fuchs, *Eur. J. Org. Chem.* **2001**, 729; f) A. Star, I. Goldberg, B. Fuchs, *J. Organomet. Chem.* **2001**, *630*, 67.

[4] a) I. J. Burden, J. F. Stoddart, *J. Chem. Soc., Perkin Trans. 1* **1975**, 666; b) I. J. Burden, J. F. Stoddart, *J. Chem. Soc., Perkin Trans. 1* **1975**, 675; c) L. Norskov, R. B. Jensen, G. Schroll, *Acta Chem. Scand.* **1983**, *B37*, 133 and previous papers in the series; d) R. Nouguier, J.-L. Gras, M. Mchich, *Tetrahedron* **1988**, *44*, 2943; e) J. F. Stoddart, *Stereochemistry of Carbohydrates*, Wiley, New York, **1971**, p. 210 and J. F. Stoddart, *Chem. Rev.* **1989**, *89*, 929.

[5] a) F. Vögtle, P. Neumann, *Synthesis* **1973**, 85 ; b) F. Vögtle, R. G. Lichtenthaler, *Synthesis* **1972**, 480; c) J. S. Bradshaw, J. Y. K. Hui, *J. Heterocycl. Chem.* **1974**, *11*, 649; d) S. G. Murray, F. R. Hartley, *Chem. Rev.* **1981**, *81*, 365; e) V. V. Litvinova, A. V. Anisimov, *Chem. Heterocycl. Comput.* **1999**, *35*, 1385.

[6] a) S. R. Cooper (Ed.), *Crown Compounds: toward future applications*, VCH, Weinheim, **1992**; b) S. R. Cooper, S. C. Rawle, *Struct. Bonding* **1990**, *72*, 1; c) S. R. Cooper, *Acc. Chem. Res.* **1988**, *21*, 141; d) R. E. Wolf, J. J. R. Hartman, J. M. E. Storey, B. M. Foxman, S. R. Cooper, *J. Am. Chem. Soc.* **1987**, *109*, 4328.

[7] a) J. Buter, R. M. Kellogg, *J. Org. Chem.* **1981**, *46*, 4481 ; b) J. J. H. Edema, H. T. Stock, M. T. J. Buter, R. M. Kellogg, W. J. J. Smeets, W. J. J. Speck, A. L. F. L. v. Bolhuis, *Angew. Chem. Int. Ed. Engl.* **1993**, *32*, 436; c) H. Xianming, R. M. Kellogg, F. Bolhuis, *J. Chem. Soc., Perkin Trans. 1* **1994**, 707; d) J. J. H. Edema, J. Buter, R. M. Kellogg, *Tetrahedron* **1994**, *50*, 2095; e) H. T. Stock, R. M. Kellogg, *J. Org. Chem.* **1996**, *61*, 3093; f) R. M. Kellogg, *Phosphorus Sulfur Silicon Relat. Elem.* **1997**, *120 and 121*, 61.

[8] a) A. J. Blake, D. W. Bruce, I. A. Fallis, S. Parsons, M. Schroeder, *J. Chem. Soc., Chem. Commun.* **1994**, 2471; b) D. Sellman, L. Zapf, *Angew. Chem. Int. Ed. Engl.* **1984**, *23*, 807; c) D. Sellman, H. J. Kremitsl, F. Knoch, *Inorg. Chim. Acta* **1994**, *225*, 163.

[9] a) V. Prautzsch, S. Ibach, F. Vögtle, *J. Incl. Phenom. Macrocyclic Chem.* **1999**, *33*, 427; b) J. Ratilainen, K. Airola, M. Nieger, M. Bohme, J. Huuskonen, K. Rissanen, *Chem. Eur. J.* **1997**, *3*, 749; c) A. Godt, S. Duda, O. Unsal, J. Thiel, A. Harter, M. Roos, C. Tschierske, S. Diele, *Chem. Eur. J.* **2002**, *8*, 5094.

[10] In **n/m** subscripts, **n** indicates the number of $–SCH_2CH_2-$ units and **m** the number of TOD-$CH_2(SCH_2CH_2)_n$ units in any oligomer or macrocycle.

[11] a) S. Otto, R. L. E. Furlan, J. K. M. Sanders, *J. Am. Chem. Soc.* **2000**, *122*, 12063; b) S. Otto, S. Kubik, *J. Am. Chem. Soc.* **2003**, *125*, 7804; c) K. R. West, K. D. Bake, S. Otto, *Org. Lett.* **2005**, *7*, 2615 and other references cited there.

[12] Y. Izumi, T. Fujita, *J. Mol. Catal. A* **1996**, *106*, 43 and earlier references there.

[13] a) L. A. Ochrymowycz, C. P. Mak, J. D. Michna, *J. Org. Chem.* **1974**, *39*, 2079; b) D. B. Rorabacher, N. E. Meagher, K. L. Juntunen, P. V. Robandt, G. H. Leggett, C. A. Salhi, B. C. Dunn, R. R. Schroeder, L. A. Ochrymowycz, *Pure Appl. Chem.* **1993**, *65*, 573.

[14] a) G. Reid, M. Schroder, *Chem. Soc. Rev.* **1990**, 239; b) M. Schroeder, *Pure Appl. Chem.* **1988**, *60*, 517.

[15] Insight II 98 program package, Molecular Simulations Inc., San Diego, CA.

[16] This is a manifestation of the dynamic behaviour of ethylene dithioglycol and its higher homologues, in: basic media, which we have touched on before[1g] and then investigated in detail, the account of which is being completed presently: S. Abramson, M. Grabarnik, S. Weinman, B. Fuchs, "On the Use of Ethylene Thioglycols in Polythiacrown Chemistry and a New Convenient Preparation of Oligoethylene Thioglycols", paper to be submitted.

[17] W. Rosen, D. H. Buseh, *Inorg. Chem.* **1970**, *9*, 262.

Received: December 1, 2006
Published Online: March 2, 2007

